Masters Thesis: Reciprocal mixing and inherent nonlinearity in N-path filters

Pieter van der Kamp

Technische Universiteit Delft

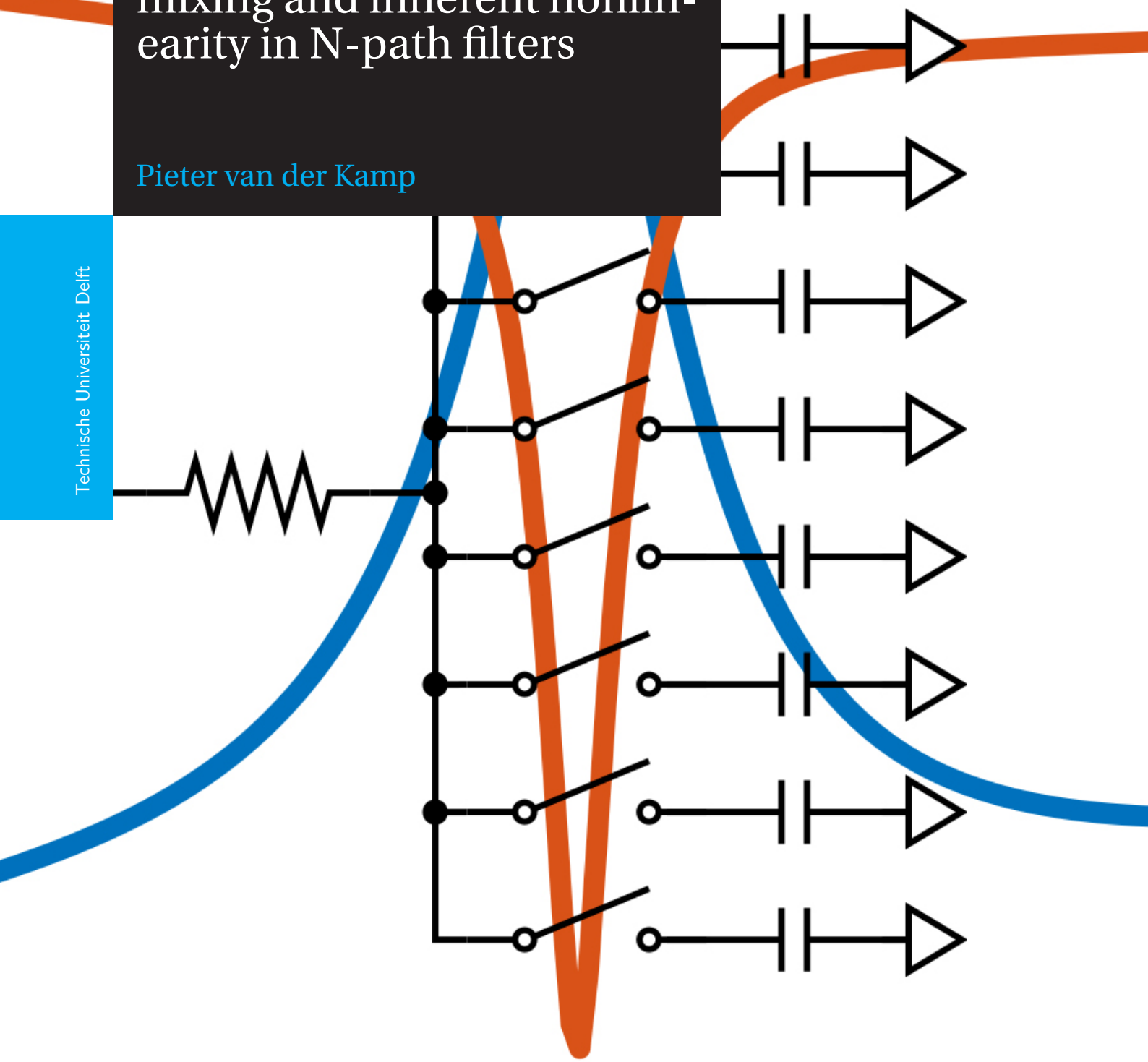

TU Delft Delft University of Technology

Challenge the future

Masters Thesis: Reciprocal mixing and inherent nonlinearity in N-path filters

by

Pieter van der Kamp

to obtain the degree of Master of Science

at the Delft University of Technology,

to be defended publicly on Friday July 8, 2022 at 13:00.

Student number:	425889	
Project duration:	September 2, 2019 – July 8, 2022	
Thesis committee:	Dr. M. Babaie,	TU Delft, supervisor
	Prof. dr. ir. L. C. N. de Vreede,	TU Delft
	Dr. D. G. Muratore,	TU Delft

An electronic version of this thesis is available at http://repository.tudelft.nl/.

TU Delft Delft University of Technology

ABSTRACT

N-path filters promise to miniaturize RF receivers by replacing various fixed off-chip filters with a single programmable on-chip filter. This research investigates some of the issues of receivers with N-path filters under strong blocker conditions: reciprocal mixing and inherent nonlinearity. First, a technique for reciprocal mixing cancellation is explored and shown to be impossible using only mixers and baseband impedances. Second, the inherent nonlinearity of both bandpass and notch N-path filters are simulated and modelled. To validate this approach, a highly linear receiver is proposed and designed in 40nm CMOS. The receiver has a bandpass common gate architecture, with a notch filter in the feedback path, improving linearity. The filter is isolated using buffers, improving LO leakage. The common gate stage is IM3 compensated to obtain good linearity (OOB IIP3 >20 dBm).

Contents

1

INTRODUCTION

1.1. N-PATH FILTERS

N-path filters, also known as M-phase filters, were first described by L.E. Franks and I. W. Sandberg [1]. They proposed a class of tunable filters, created by taking a baseband filter and periodically switching the signal to the different paths or phases of the filter. The periodic switching shifts the response of the baseband filter to the switching frequency. Later works show that this is functionally the same as having a passive mixer and baseband filter, where the mixer is used for both the downconversion and upconversion of the signal to achieve the filter response at the mixer switching frequency [2]. This is also known as mixer transparency, a characteristic feature of passive mixers.

Interest in these types of filters has increased in recent years([3], [4], [5]). Miniaturization allows n-path filters to be included on a single chip. With N-path filters, frequency-selective filters with narrow bandwidth can be realized without any inductors. Moreover, the ability to change the filter frequency is promising for today's data communications systems. If one N-path filter could replace multiple fixed-frequency the first filters in the receiver chain, cost and complexity could be greatly reduced. To achieve this, there are some tough requirements for the filter. Because the filter is the first in the chain, any signals that are received by the antenna are presented to the filter. In particular, undesired signals with large amplitude called blockers can degrade the signal by intermodulation distortion and reciprocal mixing.

1.2. RECIPROCAL MIXING

Reciprocal mixing occurs when the tone driving the mixer, the local oscillator (LO), is not pure [6]. In an ideal mixer, a blocker is downconverted with the same frequency offset as the signal of interest, preserving their relative frequency offset. A real LO has noisy sidebands that also mix with the blocker. The result is a noisy spectrum around the blocker. When the noise spectrum overlaps the wanted signal this is called reciprocal mixing. Figure 1.1 visually shows this process. If a strong blocker is present, even a low phase noise LO can result in significant blocker power inserted into the band of interest, degrading the signal-to-noise ratio. Reciprocal mixing is particularly a problem in receiver architectures with no antenna-level filtering, because the blocker is presented to the mixer without any attenuation. If antenna-level filtering is to be achieved with an N-path filter, reciprocal mixing is present in the N-path filter, since the switches of the filter implement a mixing operation. This research tries to answer the question: Is it possible to cancel reciprocal mixing in an N-path filter?

The first part of the thesis considers these questions. An existing reciprocal mixing cancellation technique is discussed. Then, the N-path filter is analysed and this analysis is verified by simulation. Next, the mechanisms in which reciprocal mixing is generated in N-path mixers are analysed and this analysis is again verified by simulation. Using the insight from these models, four ideas are proposed to cancel reciprocal mixing. These ideas are evaluated using the developed models and by simulation. The part is concluded by generalizing the results of the four reciprocal mixing cancellation ideas. From this generalization follow the conditions

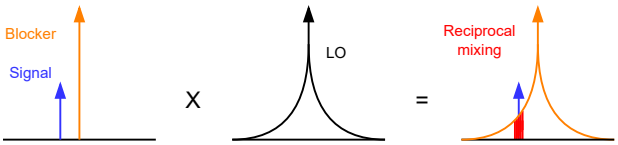

Figure 1.1: Reciprocal mixing in a blocker scenario

under which reciprocal mixing cancellation is possible.

1.3. INTERMODULATION DISTORTION

Intermodulation distortion occurs in every device which has a nonlinear transfer. Two out-of-band signals can be modulated by a nonlinear transfer, and the resulting signal could be in-band, interfering with the wanted signal. This is a problem when blockers are present. Even when the transfer is very linear, the large amplitude of the blockers causes significant intermodulation distortion.

N-path filters are constructed with NMOS used as switches. They are used in a passive way, with no DC bias current. In this setup, the transistor is biased in the linear region. An NMOS device is however not intrinsically linear, so some nonlinearity remains [7]. If a current is passed through the NMOS, the nonlinearity of the transistor generates higher order currents. These nonlinear current components then generate a voltage on the output impedance. The input and output capacitances of NMOS transistors are also not linear, and could contribute to the nonlinearity. Since the current through the transistor is dependent on both the input and output impedance, they also affect the nonlinearity. This research tries to answer the question: What factors contribute to N-path filter nonlinearity? How can this knowledge be used to design a highly linear N-path receiver?

The second part of the thesis examines these questions. Previous work on N-path nonlinearity is discussed. Then, the linearity of N-path filters is analysed and a model is developed based on this analysis. This model is verified using simulation. Next, the linearity of four receiver architectures is modeled, simulated and compared. Using the insight in N-path and receiver architecture linearity, a highly linear bandpass common gate with N-path filter is proposed. The parts of the design is discussed

2

RECIPROCAL MIXING CANCELLATION

2.1. PRIOR ART

The technique of reciprocal mixing cancellation [6] exploits the property of phase noise symmetry around the carrier to cancel reciprocal mixing. For a local oscillator (LO) with weak phase modulation, the spectrum on the upper sideband of the carrier is exactly the same as the spectrum on the lower sideband, only mirrored around the carrier and 180 degrees out of phase [8]. This is known as the narrow-band frequency modulation (NB-FM) approximation. The architecture used to exploit this property is shown in Figure 2.1. The input signal is mixed to an intermediate frequency (IF) and filtered to reject the upconverted signals and leave just the downconverted signal, blocker, and noise from reciprocal mixing. A phase-locked loop (PLL) is used to lock on to the blocker. The output frequency of this PLL is two times the blocker frequency, without reciprocal mixing noise from the LO. The IF signal is then mixed with this PLL output, effectively mirroring the spectrum around the blocker. This also mirrors the reciprocal mixing spectrum. This reconstructed reciprocal mixing is added to the IF signal, cancelling out the reciprocal mixing term. If the blocker consists of a single tone, the PLL and mixer of the auxiliary path can be replaced with a third-order nonlinearity, since this mixes a signal with the second harmonic of itself.

This method works well. For a single tone blocker, it is also easy to implement. For a realistic, modulated blocker, however, it needs a PLL that is fast enough to track the blocker. The phase noise of this PLL must not be worse than that of the LO of the downconversion mixer in the main RX path, negating the RM cancellation. Because the PLL works at IF, its requirements are relaxed with respect to the main LO.

N-path filters also suffer from reciprocal mixing, since the switches of the N-path filter implement a mixing operation. On the other hand, N-path filters have unique properties like impedance upconversion. The question arises: can the properties of N-path filters be used to cancel reciprocal mixing? To answer this question, the N-path filter is analysed. Using this analysis, several potential solutions are investigated. The analysis is verified using simulation.

2.2. N-PATH FILTER

The mathematical analysis of the N-path filter can yield complicated expressions. To gain a more intuitive understanding of the N-path filter, a graphical analysis is presented. This analysis assumes the switches are ideal. Also, capacitors are chosen as the load impedance. Figure 2.2 shows an example of a 4-path filter with these properties.

When one of the switches is closed, the corresponding capacitor is charged or discharged through the resistor. For the filter to work, the time constant of this charging must be much higher than the time the switch is closed ($RC >> T_{on}$). If a sinusoidal signal with the same period as the switching signals is presented to the system, each capacitor will be charged by the same part of the signal each cycle. Figure 2.3 shows this visually. The capacitors will settle to a voltage equal to the average of the part of the input signal they are presented

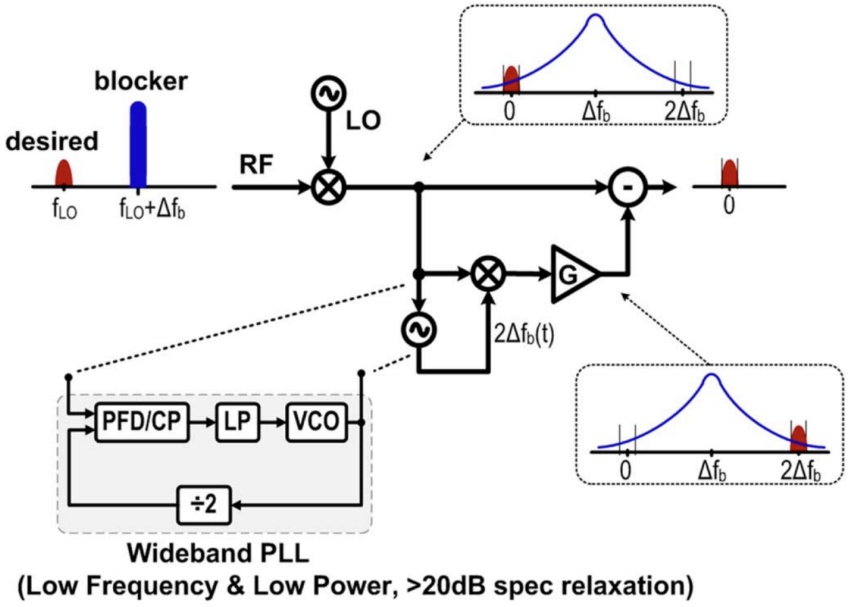

Figure 2.1: Block diagram of the reciprocal mixing cancelling receiver from [6].

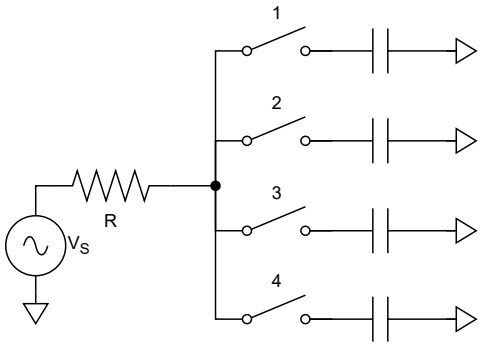

Figure 2.2: 4-path bandpass filter.

with. When settled, little current will be drawn by the capacitors, the signal voltage on the output remains close to the input voltage.

When a signal with a higher frequency is presented to the filter, the capacitors are presented to a different part of the signal each cycle. This causes the capacitors to be charged and discharged continuously, as illustrated in Figure 2.4 The required current creates a voltage drop across the resistor, reducing the signal amplitude. This also happens for a signal with a lower frequency than the switching signals.

If a signal with exactly twice the switching frequency is presented to the filter, the same happens as with a signal equal to the switching frequency: the capacitor voltages settle to a dc value, as illustrated in Figure 2.5. This shows that the filter response is not only present at the switching frequency, but also at harmonics of this frequency.

2.2.1. ANALYSIS

First, the N-path filter will be analysed without reciprocal mixing. The goal is to find an expression for the linear transfer from the input to each node in the circuit. These results can be used as a starting point for the reciprocal mixing analysis. To simplify the analysis, the symmetry between the paths is exploited. All

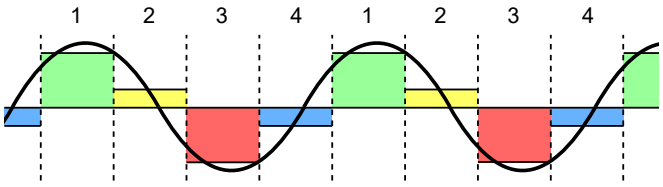

Figure 2.3: Response of 4-path bandpass filter to a signal with frequency equal to the switching frequency.

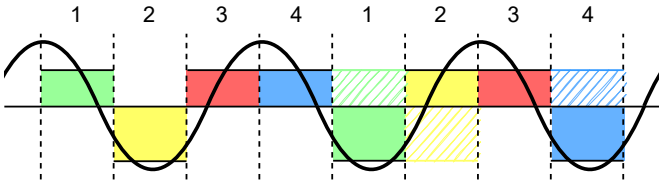

Figure 2.4: Response of 4-path bandpass filter to a signal with frequency higher than the switching frequency.

switches and load impedances are the same, the only difference is a phase shift in the signal driving the switches. This allows replacing the switched impedances with an equivalent impedance, as seen from the input. The switch is modeled by a resistor whose value is equal to the on-resistance of the transistor used for the switch operation.

To continue with the analysis, several more assumptions must be made. First, the input signal contains only tones around f_{LO}, specifically between $0.5f_{LO}$ and $1.5f_{LO}$. Secondly, the load impedance Z_L is lowpass, such that only the baseband components of the voltage on Z_L are important. Voltage components on frequencies higher than $0.5f_{LO}$ are treated as zero. However, there are still current components on these higher frequencies. The input signal also mixes with the harmonics of the LO frequency. Because these currents produce no voltage, it represents a loss. This effect can also be observed from Figure 2.3. The combined baseband signals (represented by the colored blocks) do not track the input perfectly, because there are only a N samples per signal period. The difference between the input signal and sampled signal is lost. This loss can be modeled by a resistor. This resistor is in parallel with load impedance and can be absorbed in the load impedance. The expressions for this resistor (R_{sh}) and the load impedance as seen from the input ($Z_{L,RF}$) are adapted from [9]. Equation 2.2 shows both the baseband and RF impedance with absorbed R_{sh}. The term γ is only dependent on the number of paths of the filter.

$$\begin{aligned} R_{sh,BB} &= \frac{N}{1-\gamma^2}(R_S + R_{sw}) \\ R_{sh,RF} &= \frac{\gamma^2}{N} R_{sh,BB} \end{aligned} \tag{2.1}$$

$$\begin{aligned} Z_{BB}(\omega) &= \frac{Z_L(\omega) R_{sh,BB}}{Z_L(\omega) + R_{sh,BB}} \\ Z_{L,RF}(\omega) &= \frac{\gamma^2}{N} Z_L(\omega - \omega_{LO}) \\ Z_{RF}(\omega) &= \frac{\gamma^2}{N} Z_{BB}(\omega) = \frac{\frac{\gamma^2}{N} Z_L(\omega - \omega_{LO}) R_{sh,RF}}{\frac{\gamma^2}{N} Z_L(\omega - \omega_{LO}) + R_{sh,RF}} = \frac{Z_{L,RF}(\omega) R_{sh,RF}}{Z_{L,RF}(\omega) + R_{sh,RF}} \end{aligned} \tag{2.2}$$

$$\gamma = \frac{N}{\pi} \sin\left(\frac{\pi}{N}\right) \tag{2.3}$$

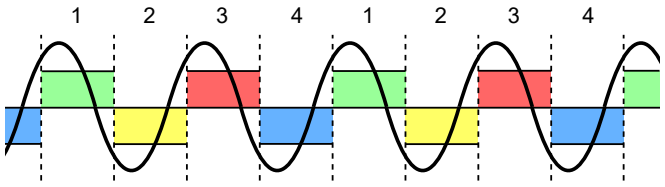

Figure 2.5: Response of 4-path bandpass filter to a signal with frequency two times the switching frequency.

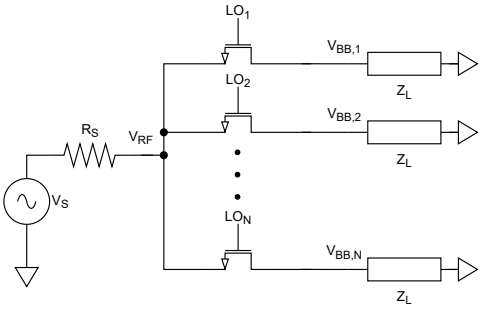

(a) N-path filter.

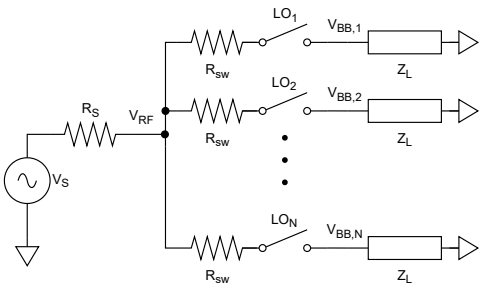

(b) N-path filter with transistors modeled as resistors and ideal switches.

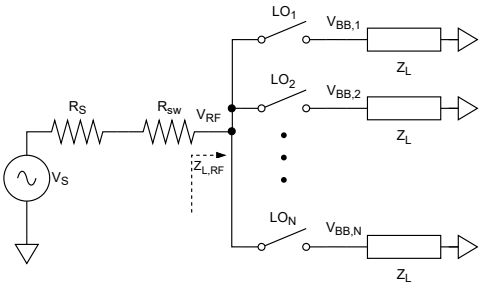

(c) Simplified model for nonoverlapping LO phases.

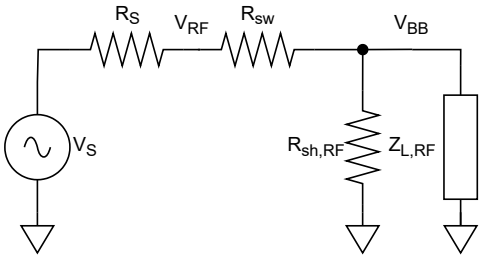

(d) Single-phase equivalent with equivalent impedance and resistor modeling losses by mixing with harmonics

Figure 2.6: Derivation of a simplified schematic for analysis of the N-path filter

From equation 2.1, it is clear that increasing the number of paths reduces the loss associated with LO harmonics. For filters with a high number of phases, R_{sh} can be neglected. For a purely capacitive Z_L and a high number of phases, equation 2.2 reduces to $Z_{L,RF} = \frac{\gamma^2}{j(\omega-\omega_{LO})NC_L}$. This shows that increasing the number of phases does not change the total amount of capacitance required for a certain filter bandwidth.

Now that all the impedances in the circuit are known, the voltage and current on the RF side can be calculated.

$$I_{RF}(\omega) = \frac{V_S}{R_S + R_{sw} + Z_{RF}(\omega)} \tag{2.4}$$

$$V_{RF}(\omega) = V_S \frac{R_{sw} + Z_{RF}(\omega)}{R_S + R_{sw} + Z_{RF}(\omega)} \tag{2.5}$$

The signals on the baseband side can not be directly determined from the simplified circuit. The mixer gain must be taken into account. Also, these signals are at other frequencies than the input signal, downconverted to baseband. The expressions for I_{BB} and V_{BB} refer to the signal on a single phase of the filter.

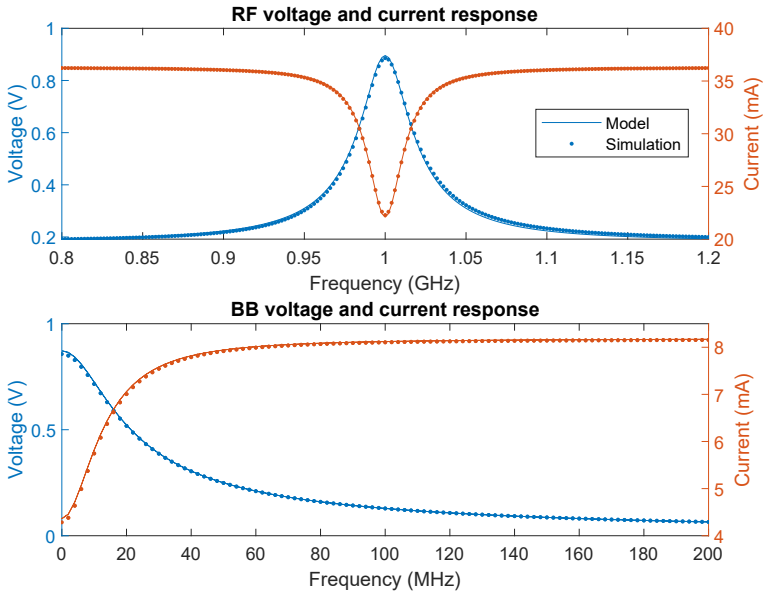

Figure 2.7: Comparison of the N-path model with simulation data

$$\begin{aligned} V_{BB}(\omega) &= \frac{\gamma}{N} Z_{BB}(\omega) I_{RF}(\omega + \omega_{LO}) \\ &= \frac{\gamma}{N} V_S \frac{Z_{BB}(\omega)}{R_S + R_{sw} + Z_{RF}(\omega + \omega_{LO})} \end{aligned} \tag{2.6}$$

$$\begin{aligned} I_{BB}(\omega) &= \frac{V_{BB}(\omega)}{Z_L(\omega)} \\ &= \frac{\gamma}{N} V_S \frac{1}{Z_L(\omega)} \frac{Z_{BB}(\omega)}{R_S + R_{sw} + Z_{L,RF}(\omega + \omega_{LO})} \end{aligned} \tag{2.7}$$

2.2.2. VERIFICATION

To verify the developed model, a 4-path filter was simulated using pss+pac in Cadence Spectre. The switching frequency is 1 GHz. The source resistance is 50 Ω, the swich on resistance 5 Ω and the load impedance constists of a 200 Ω resistor in parallel with a 100 pF capacitor. The results, shown in Figure 2.7, show that the model accurately predicts the behaviour of the filter.

2.3. RECIPROCAL MIXING IN N-PATH FILTERS

2.3.1. ANALYSIS

The analysis of reciprocal mixing in N-path filters is done as follows. First, a wanted signal and a blocker are presented to the N-path filter, represented by single tones. Using the equations for transfer of a signal without reciprocal mixing, the components of the wanted signal and blocker are evaluated for both nodes in the circuit. Knowing the signal and blocker components on each node, reciprocal mixing terms can be determined. To simplify this analysis, the phase noise is represented by a single spur. The full solution can then be obtained by a convolution of the spur with a phase noise spectrum. This is possible because phase noise is a weak modulation, and can be modeled as an infinite sum of uncorrelated spurs [8]. There are two

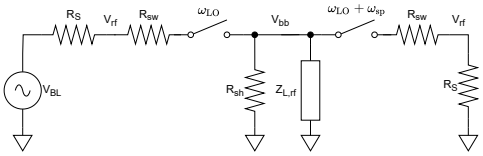

(a) Reciprocal mixing method A:
reciprocal mixing generated during upconversion

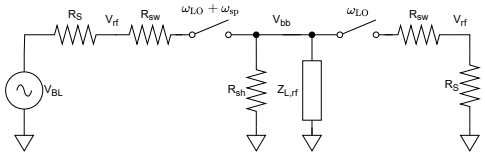

(b) Reciprocal mixing method B:
reciprocal mixing generated during downconversion

Figure 2.8: Two mechanisms that generate reciprocal mixing terms

ways in which reciprocal mixing is generated. Either by mixing the blocker signal at baseband with an LO spur, or by mixing the blocker signal at RF with an LO spur. Figure 2.8 shows both methods. The circuit of Figure 2.6d is copied and mirrored around the baseband impedance, to separate the up- and downconversion step of the mixer.

Everything necessary to solve the circuits of Figure 2.8 is known, except the behaviour of the switches. To find this, first the LO is described, with a single tone modeling the phase noise. β is the phase modulation factor and determines the strength of the phase noise.

$$\begin{aligned} v_{LO}(t) &= A_{LO}\cos\left(\theta_{LO}(t)\right) \\ \theta_{LO}(t) &= 2\pi f_{LO}t + \beta\phi_n(t) \\ \phi_n(t) &= \sin(2\pi f_{sp}t) \end{aligned} \tag{2.8}$$

From the LO, the switch operation is derived. When the switch is closed, the input current is equal to the output current and the input voltage is equal to the output voltage. When the switch is open, the currents are 0. This is modeled by the variable $S(t)$. It is 0 when open and 1 when closed.

$$s(t) = \begin{Bmatrix} 1 & |\theta_{LO}(t) + k2\pi| < \frac{\pi}{N} \\ 0 & |\phi_{LO}(t) + k2\pi| > \frac{\pi}{N} + k2\pi \end{Bmatrix}, -\pi + k2\pi < t < \pi + k2\pi \tag{2.9}$$

The switch operation can be split into an ideal part s_i and an error part s_ϵ, which arises because of the phase noise. The ideal switch is a square wave with duty cycle $\frac{1}{N}$. For small β, the weak PM approximation can be made. The errors are assumed to be very small and can therefore be modeled as delta pulses on the edges of the ideal switching signal, as illustrated by Figure 2.9.

$$\begin{aligned} s(t) &= s_0(t) + s_\epsilon(t) \\ s_0(t) &= \sum_{k=-\infty}^{\infty} \Pi\left(\frac{N\omega_{LO}}{2\pi}(t - kN)\right) \\ s_\epsilon(t) &\approx \frac{\beta}{\omega_{LO}}\sin\left(\omega_{sp}t\right) \times \\ &\quad \sum_{k=-\infty}^{\infty} \delta\left(t - \frac{2\pi k}{\omega_{LO}} + \frac{pi}{N\omega_{LO}}\right) - \delta\left(t - \frac{2\pi k}{\omega_{LO}} + \frac{\pi}{N\omega_{LO}}\right) \end{aligned} \tag{2.10}$$

This equation is transformed to the frequency domain using a Fourier transform, shown in equation 2.11.

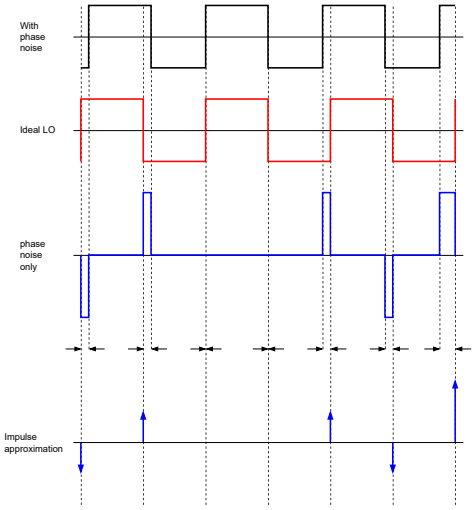

Figure 2.9: Approximating phase noise on a square wave in time domain with delta pulses

$$
\begin{aligned}
s(t) \xrightarrow{\mathcal{F}} S(\omega) &= S_0(\omega) + S_\epsilon(\omega) \\
S_0(\omega) &= \frac{1}{N}\delta(\omega) + \sum_{n=-\infty}^{\infty} a_n \delta(\omega - n\omega_{LO}) \\
S_\epsilon(\omega) &= \beta \sum_{n=-\infty}^{\infty} n a_n \left(\delta(\omega - \omega_{sp} - n\omega_{LO}) - \delta(\omega + \omega_{sp} - n\omega_{LO})\right) \\
a_n &= \frac{1}{n\pi}\sin\left(\frac{n\pi}{N}\right)
\end{aligned}
\tag{2.11}
$$

Only the first harmonic ($n = \pm 1$) is of importance, because of the assumptions used in this analysis: Z_L is lowpass, and there are no input signals around LO harmonics. The previous equations described only one phase. Since the phases are nonoverlapping, the total result can be obtained by multiplying with the number of phases N to get a value that can be used in the simplified schematic of Figure 2.8. The remaining terms are all around the LO frequency, as equation 2.12 shows. Since $N \cdot a_1$ is equal to γ used in the earlier equations, this term will be used from now on.

$$
\begin{aligned}
S_{0,N}(\omega) =& N a_1 \left(\delta(\omega - \omega_{LO}) + \delta(\omega + \omega_{LO})\right) \\
S_{\epsilon,N}(\omega) =& N a_1 \beta \big(\delta(\omega - \omega_{sp} - \omega_{LO}) - \delta(\omega + \omega_{sp} - \omega_{LO}) \\
& - \delta(\omega - \omega_{sp} + \omega_{LO}) + \delta(\omega + \omega_{sp} + \omega_{LO})\big) \\
a_1 =& \frac{1}{\pi}\sin\left(\frac{\pi}{N}\right)
\end{aligned}
\tag{2.12}
$$

Mechanism A (Figure 2.8a) shows reciprocal mixing added during upconversion of the baseband blocker signal. Knowing the linear transfer of the input to the voltage at baseband from equation 2.6, the blocker voltage at baseband is known.

$$
V_{BB,bl}(\omega_{bl}) = \frac{\gamma}{N} V_{bl} \frac{Z_{BB}(\omega_{bl})}{R_S + R_{sw} + Z_{L,RF}(\omega_{bl} + \omega_{LO})} \tag{2.13}
$$

This voltage is mixed with the phase noise, represented by S_ϵ to RF. The terms of S_ϵ can be separated into two groups, two with $+\omega_{sp}$ and with $-\omega_{sp}$. Only one is needed, since only one term causes the reciprocal mixing

term to be on top of the wanted signal. It does not matter which term is chosen, as long as the analysis for the other reciprocal mixing mechanism uses the correct term, so the mixing ends up at the same frequency. In this analysis the terms with $-\omega_{sp}$ are used. Also, both equations contain terms for upconversion and for downconversion. Because in this mechanism, the reciprocal mixing is produced during upconversion, the other terms can be ignored. The mixing operation is a convolution, and since S_ϵ only has terms multiplied with unit impulses, it corresponds to a shift in frequency and a scaling.

$$\begin{aligned} V_{RF,rm,A}(\omega_{bl}-\omega_{sp}) &= \frac{R_S}{R_S+R_{sw}} V_{BB,bl} * S_{\epsilon,N}(\omega_{bl}) \\ &= -\beta V_{bl} \frac{R_S}{R_S+R_{sw}} \frac{Z_{RF}(\omega_{bl})}{R_S+R_{sw}+Z_{L,RF}(\omega_{bl})} \end{aligned} \tag{2.14}$$

Mechanism B (Figure 2.8b) shows reciprocal mixing added during downconversion of the RF blocker signal. A part of the RF blocker current is mixed with the phase noise to the baseband reciprocal mixing current. At the RF side, this current is at the blocker frequency, but at the baseband side, it is at the reciprocal mixing frequency. This changes the RF input impedance as 'seen' by this current. The RF blocker current from equation 2.4 is adapted to this fact by changing the frequency of the RF equivalent of the load impedance.

$$I_{RF,bl}(\omega_{bl}) = \frac{V_{bl}}{R_S+R_{sw}+Z_{RF}(\omega_{bl}-\omega_{sp})} \tag{2.15}$$

This current is mixed with the phase noise, just as in mechanism A. Only now the signal is downconverted instead of upconverted.

$$\begin{aligned} V_{BB,rm}(\omega_{bl}-\omega_{sp}) &= \left(I_{RF,bl}(\omega_{bl}) * S_{\epsilon,N}\right) Z_{BB}(\omega_{bl}-\omega_{sp}) \\ &= \beta\frac{\gamma}{N} V_{bl} \frac{Z_{BB}(\omega_{bl}-\omega_{sp})}{R_S+R_{sw}+Z_{RF}(\omega_{bl}-\omega_{sp}-\omega_{LO})} \end{aligned} \tag{2.16}$$

This voltage is upconverted again to RF. This time the equation for the ideal switch without reciprocal mixing is used to find the component of reciprocal mixing on RF side due to mechanism B.

$$\begin{aligned} V_{RF,rm,B}(\omega_{bl}-\omega_{sp}) &= \frac{R_S}{R_S+R_{sw}} V_{BB,bl}(\omega_{bl}-\omega_{LO}) * S_0(\omega_{LO}) \\ &= \beta V_{bl} \frac{R_S}{R_S+R_{sw}} \frac{Z_{RF}(\omega_{bl}-\omega_{sp})}{R_S+R_{sw}+Z_{RF}(\omega_{bl}-\omega_{sp})} \end{aligned} \tag{2.17}$$

Finishing the analysis, the components from mechanism A and B are combined.

$$\begin{aligned} &V_{RF,rm}(\omega_{bl}-\omega_{sp}) = V_{RF,rm,A} + V_{RF,rm,B} \\ &= \beta V_{bl} \frac{R_S}{R_S+R_{sw}} \left(\frac{Z_{RF}(\omega_{bl}-\omega_{sp})}{R_S+R_{sw}+Z_{RF}(\omega_{bl}-\omega_{sp})} - \frac{Z_{RF}(\omega_{bl})}{R_S+R_{sw}+Z_{RF}(\omega_{bl})} \right) \end{aligned} \tag{2.18}$$

$$\begin{aligned} &I_{RF,rm}(\omega_{bl}-\omega_{sp}) = -\frac{V_{RF,rm}}{R_S} \\ &= \beta V_{bl} \frac{1}{R_S+R_{sw}} \left(\frac{Z_{RF}(\omega_{bl}-\omega_{sp})}{R_S+R_{sw}+Z_{RF}(\omega_{bl}-\omega_{sp})} - \frac{Z_{RF}(\omega_{bl})}{R_S+R_{sw}+Z_{RF}(\omega_{bl})} \right) \end{aligned} \tag{2.19}$$

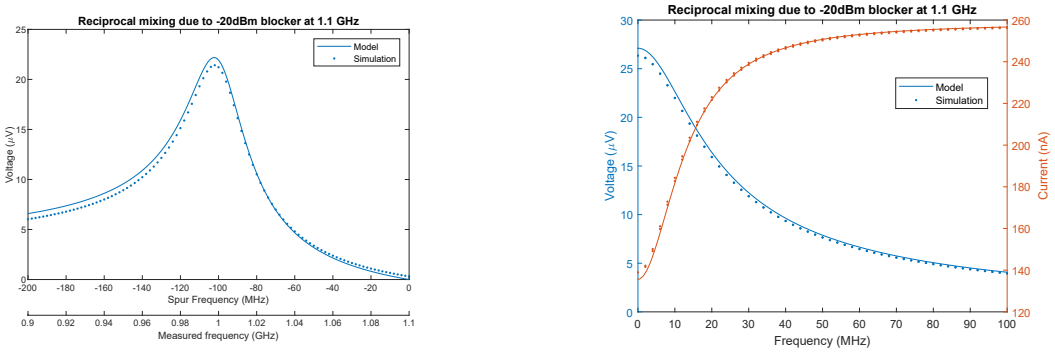

Figure 2.10: Comparison of the N-path reciprocal mixing model with simulation data

2.3.2. VERIFICATION

The results of the analysis are verified using the same setup as used for the verification of the signal response. The spur frequency offset from the filter center frequency was swept, while keeping its amplitude constant. This is equivalent to an LO with a flat phase noise spectrum. A -20dBm blocker at 1.1 GHz is presented to the filter, which has a center frequency of 1 GHz. The resulting voltages are compared to the model in Figure 2.10. At the baseband side of the filter, the response is just a scaled version of the signal response of the filter. On the RF side of the filter, at the blocker frequency (1.1 GHz), there is no reciprocal mixing. The reciprocal mixing term peaks around the filter center frequency. Far away from the blocker it settles to a constant value. This corresponds with the model, which has a constant term and a upconverted baseband term which cancel out at the blocker frequency. This simulation data does not correspond as precisely with the model as the data in Figure 2.7. This could be due to non-linear effects of the phase modulator, which is assumed to be linear in the analysis. Still, the model predicts the reciprocal mixing very well.

2.4. RECIPROCAL MIXING CANCELLATION

Using the insight of the reciprocal mixing analysis, receiver architectures are proposed which are expected to have possibilities for reciprocal mixing cancellation. In total, 4 ideas are explored. Each idea is analysed using the equations for reciprocal mixing. The setup of these analyses is the same for each idea: a signal and blocker are presented to the system, represented by single tones. The LO phase noise is modeled as a spur with frequency $f_{sp} = f_{bl} - f_s$, producing an reciprocal mixing term on top of the desired frequency. Lastly, the conclusions of the analysis are verified with simulation.

2.4.1. IDEA 1: TWO PATHS

The first proposed method for RM cancellation involves two N-path filters connected to the same source. The filters are similar but have different baseband impedances. It is expected that the baseband impedance affects the reciprocal mixing and the wanted signal differently, because the blocker is attenuated by the baseband impedance while the signal is not. This creates two downconverted signals with different ratios between signal and RM. If these signals are combined in the right ratio, the reciprocal mixing can be cancelled while retaining the wanted signal. Figure 2.11 shows the proposed method.

This idea can be analysed using the previously derived equations, using the setup mentioned before. Equation 2.16 is used to determine the reciprocal mixing voltage and signal voltage of both paths. Since $f_{sp} = f_{bl} - f_s$ for this analysis, $f_{bl} - f_{sp}$ is replaced with f_s.

$$V_{BB,rm,1}(\omega_s) = \beta \frac{\gamma}{N} V_{bl} \frac{Z_{BB,1}(\omega_s)}{R_{S,1} + R_{sw,1} + Z_{RF,1}(\omega_s + \omega_{LO})} \tag{2.20}$$

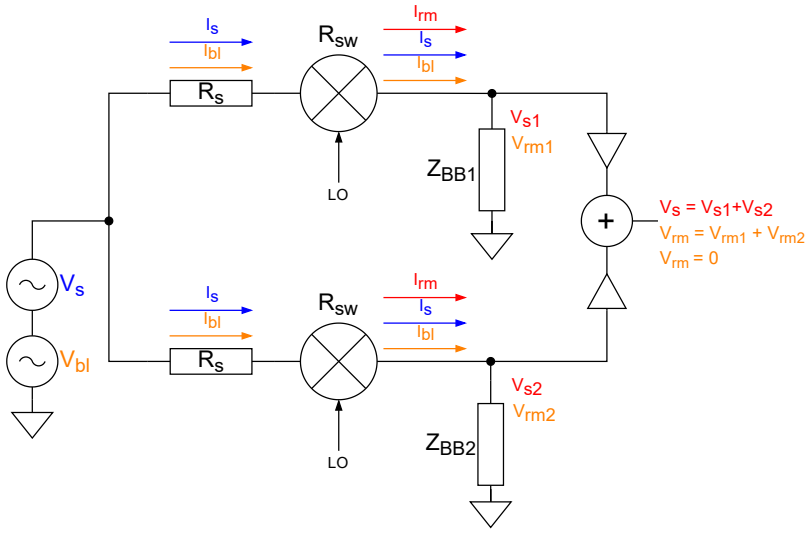

Figure 2.11: Reciprocal mixing cancellation using two paths

$$V_{BB,1} = \frac{\gamma}{N} V_s \frac{Z_{BB,1}(\omega_s)}{R_{S,1} + R_{sw,1} + Z_{RF,1}(\omega_s + \omega_{LO})} \tag{2.21}$$

The ratio between $V_{BB,rm,1}$ and $V_{BB,1}$ is calculated in equation 2.22. This shows that the ratio between wanted signal and reciprocal mixing is not dependent on impedance values in the circuit, only on the signal and blocker power and the LO phase noise amplitude, represented by β.

$$\frac{V_{BB,rm,1}}{V_{BB,1}} = \frac{\beta V_{bl}}{V_s} \tag{2.22}$$

This conclusion is verified using simulation of two 4-path filters. The parameters are: β=1m, f_{LO}=1 GHz, $R_{S,1}$=50Ω, $R_{S,2}$=100Ω, $R_{sw,1}$=5Ω, $R_{sw,2}$=10Ω, $R_{L,1}$=200Ω, $R_{L,2}$=100Ω, $C_{L,1}$=100 pF and $C_{L,2}$=400 pF. The outputs were summed such that there is no reciprocal mixing at 0 Hz. Figure 2.12 shows that this means there is also no signal at this frequency. At any frequency, the ratio between reciprocal mixing and wanted signal is equal to β.

2.4.2. IDEA 2: RM INJECTION

The second proposed method for RM cancellation again involves two N-path filters. This time, the paths are identical. Voltage from the first path is injected as a current in the second path. The transconductance controlling this current is scaled to cancel the signal at the output of the second N-path filter. Because the paths are identical, this scaling is constant over the whole bandwidth of the filter.

The analysis of this setup starts with the upper path. The signal, blocker and reciprocal mixing voltages on the RF node of this path are shown in equation 2.23.

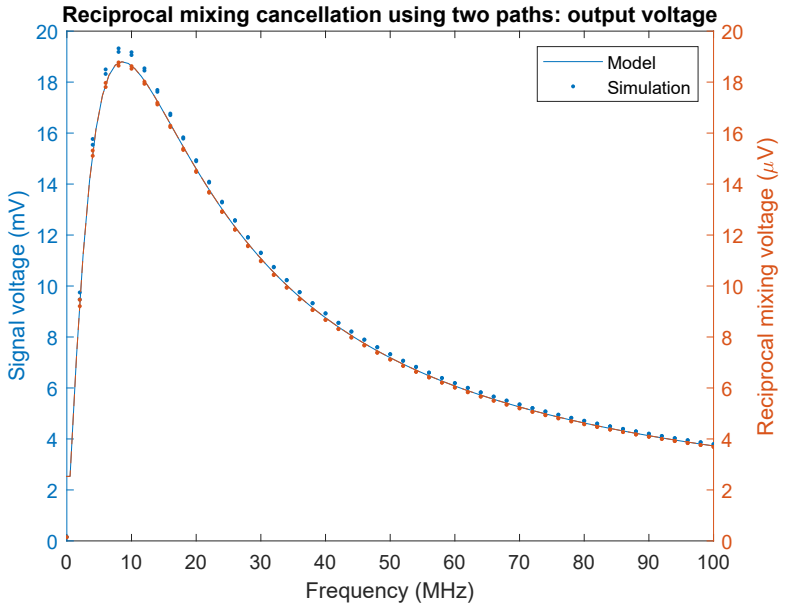

Figure 2.12: Simulation of reciprocal mixing cancellation idea 1

$$
\begin{aligned}
V_{RF,s,1}(\omega_s) &= V_s(\omega_s)\frac{Z_{RF}(\omega_s)+R_{sw}}{R_S+R_{sw}+Z_{RF}(\omega_s)} \\
V_{RF,bl,1}(\omega_{bl}) &= V_{bl}(\omega_{bl})\frac{Z_{RF}(\omega_{bl})+R_{sw}}{R_S+R_{sw}+Z_{RF}(\omega_{bl})} \\
V_{RF,rm,1} &= \beta V_{bl}(\omega_s)\frac{R_S}{R_S+R_{sw}}\times \\
&\quad \left(\frac{Z_{RF}(\omega_s)}{R_S+R_{sw}+Z_{RF}(\omega_s)}-\frac{Z_{RF}(\omega_{bl})}{R_S+R_{sw}+Z_{RF}(\omega_{bl})}\right)
\end{aligned}
\tag{2.23}
$$

These signals are injected into the second path. The transconductance delivering this current is scaled such that the signal current is cancelled at the filter center frequency, which is equal to the switching frequency f_{LO}. Its value is calculated in equation 2.25

$$
\begin{aligned}
I_{RF,s,2}(\omega_s) &= \frac{V_s}{R_S+R_{sw}+Z_{RF}(\omega_s)}+g_m V_{RF,s} \\
I_{RF,bl,2}(\omega_{bl}) &= \frac{V_{bl}}{R_S+R_{sw}+Z_{RF}(\omega_{bl})}+g_m V_{RF,bl}
\end{aligned}
\tag{2.24}
$$

$$
g_m = -\frac{I_{RF,s,2}(\omega_{LO})}{V_{RF,s,1}(\omega_{LO})} = -\frac{1}{R_{sw}+Z_{RF}(\omega_{LO})} \tag{2.25}
$$

The RF signal current is completely cancelled at the filter center frequency, and partially in band. The blocker current also is partially cancelled, but much less than the signal. With the RF currents known, the baseband voltages can be calculated. The calculation of $V_{BB,rm,2}$ requires extra attention, as not only the blocker current causes reciprocal mixing voltage at baseband, but also the reciprocal mixing current injected from the first path. It yields a complicated expression which can be manipulated into the form shown in equation 2.26.

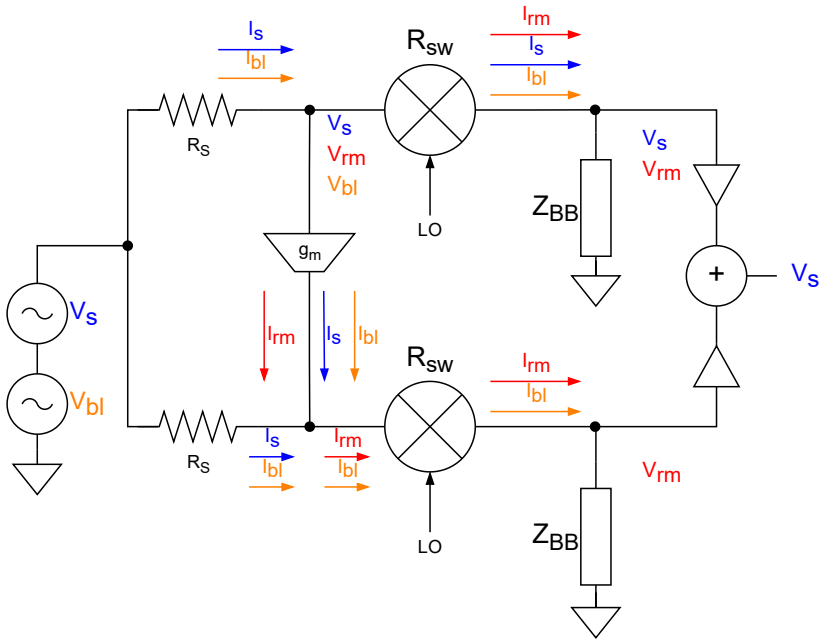

Figure 2.13: Reciprocal mixing cancellation using RM injection

$$
\begin{aligned}
V_{BB,s,2}(\omega_s-\omega_{LO}) &= \frac{Z_{L,RF}(\omega_s)}{\gamma} I_{RF,s}(\omega_s) \\
&= \frac{V_s}{\gamma} \frac{Z_{L,RF}(\omega_s}{R_S+R_{sw}+Z_{L,RF}(\omega_s)} \left(1-g_m(R_{sw}+Z_{L,RF}(\omega_s)\right) \\
V_{BB,bl,2}(\omega_{bl}-\omega_{LO}) &= \frac{Z_{L,RF}(\omega_{bl})}{\gamma} I_{RF,bl}(\omega_{bl}) \\
&= \frac{V_{bl}}{\gamma} \frac{Z_{L,RF}(\omega_{bl}}{R_S+R_{sw}+Z_{L,RF}(\omega_{bl})} \left(1-g_m(R_{sw}+Z_{L,RF}(\omega_{bl})\right) \\
V_{BB,rm,2}(\omega_s-\omega_{LO}) &= \frac{\beta}{\gamma} Z_{L,RF}(\omega_s) I_{RF,bl,2}(\omega_s) + \frac{g_m}{\gamma} Z_{L,RF}(\omega_s) V_{RF,rm,1}(\omega_s) \\
&= \frac{\beta}{\gamma} V_{bl} \frac{Z_{L,RF}(\omega_s)}{R_S+R_{sw}+Z_{L,RF}(\omega_s)} \left(1+g_m(R_s w+Z_{L,RF}(\omega_s))\right)
\end{aligned}
\tag{2.26}
$$

By dividing the reciprocal mixing voltage by the signal voltage at baseband in equation 2.27, it becomes clear that this method has not isolated the reciprocal mixing term. Cancelling the signal also cancelled reciprocal mixing, which means that this signal cannot be used to remove reciprocal mixing from the first path.

$$
\frac{V_{BB,rm,2}}{V_{BB,s,2}} = \frac{\frac{\beta}{\gamma} V_{bl} \frac{Z_{L,RF}(\omega_s)}{R_S+R_{sw}+Z_{L,RF}(\omega_s)} \left(1+g_m(R_s w+Z_{L,RF}(\omega_s)\right)}{\frac{V_{bl}}{\gamma} \frac{Z_{L,RF}(\omega_s)}{R_S+R_{sw}+Z_{L,RF}(\omega_s)} \left(1+g_m(R_s w+Z_{L,RF}(\omega_s)\right)} = \beta \tag{2.27}
$$

The results are verified using simulation of two identical 4-path filters. The parameters are: β=1m, f_{LO}=1 GHz,R_S=50Ω,R_{sw}=5Ω,R_L=200Ω and C_L=100 pF. The transconductance was scaled such that the signal is cancelled at the input of the second phase. Figure 2.14a shows that the signal is cancelled at the filter center frequency, while the reciprocal mixing term is nonzero. After downconversion, the situation is different. Figure 2.14b shows no signal at 0Hz, but also no reciprocal mixing. At baseband, the ratio between reciprocal mixing and wanted signal is equal to β for every frequency.

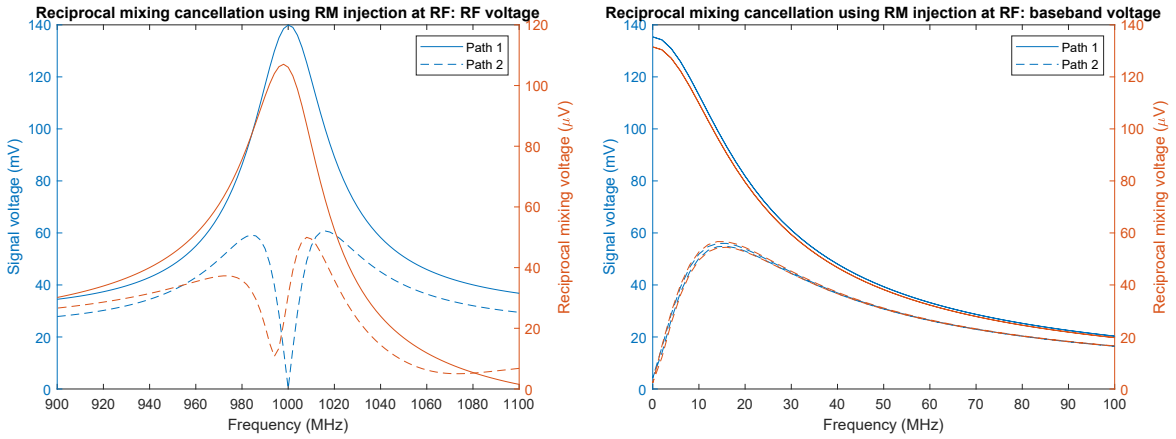

(a) RF signals

(b) Baseband signals

Figure 2.14: Simulation of reciprocal mixing cancellation idea 2

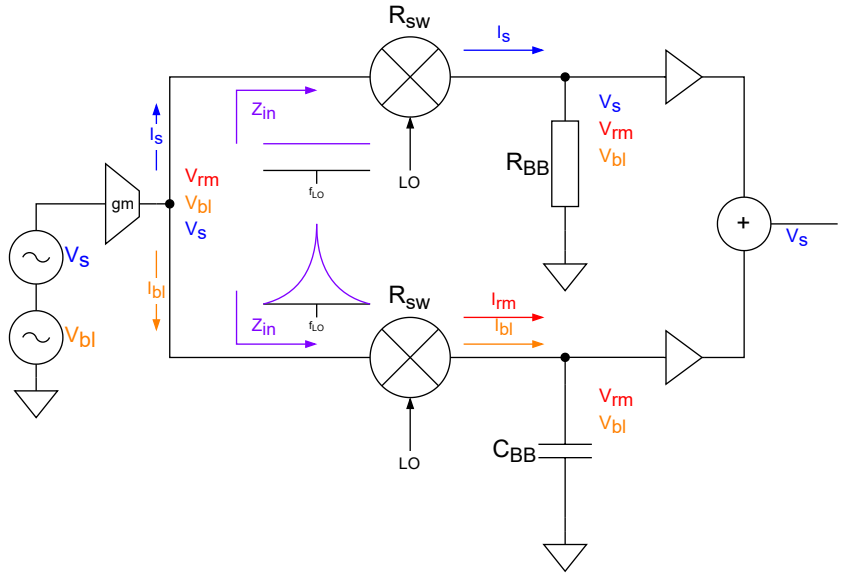

Figure 2.15: Reciprocal mixing cancellation with a blocker sink

2.4.3. IDEA 3: BLOCKER SINK

This idea involves splitting the N-path filter in two: one with a resistor as baseband impedance, and one with a capacitor. The second path sinks the blocker current since its input impedance is much lower at blocker frequencies. This filter also generates the reciprocal mixing term. The first path sinks the signal current and converts it to a voltage on the baseband impedance, with no reciprocal mixing since there is no blocker current.

For the analysis, both the upper and lower path impedance as seen from the RF side must be known. For the upper path, equation 2.2 cannot be used because this impedance is not lowpass. Instead, it is just a switched resistor, and the impedance as seen from the RF side is equal to the resistance of one path. While analysing the lower path, the complete upper path can be replaced by a resistor with value $R_{sw} + R_L$. This resistor can the be absorbed into R_S with the use of source transformations. The results of these transformations are

shown in equation 2.28.

$$\begin{aligned} R_{S,t} &= R_S \frac{(R_{sw}+R_L)}{R_S+R_{sw}+R_L} \\ V_{S,t} &= V_S \frac{(R_{sw}+R_L)}{R_S+R_{sw}+R_L} \end{aligned} \tag{2.28}$$

With the circuit transformed into the same format as the previously analysed circuits, the RF voltages of the blocker and signal can be easily calculated with the known equations. To make the equations more legible, a transfer function from the original input to the RF node is defined in equation 2.29.

$$H_{RF}(\omega) = \frac{V_{RF}}{V_S} = \frac{R_{sw}+R_L}{R_S,+R_{sw}+R_L} \frac{R_{sw}+Z_{RF}(\omega)}{R_{S,t}+R_{sw}+Z_{RF}(\omega)} \tag{2.29}$$

$$\begin{aligned} V_{RF,s}(\omega_s) &= V_s H(\omega_s) \\ V_{RF,bl}(\omega_{bl}) &= V_{bl} H(\omega_s) \end{aligned} \tag{2.30}$$

The baseband voltages of the upper branch can be calculated from these voltages, because the RF node of both paths are connected.

$$\begin{aligned} V_{BB,s}(\omega_s) &= \frac{V_s}{\gamma} \frac{R_L}{R_{sw}+R_L} H(\omega_s+\omega_{LO}) \\ V_{BB,bl}(\omega_{bl}) &= \frac{V_{bl}}{\gamma} \frac{R_L}{R_{sw}+R_L} H(\omega_{bl}+\omega_{LO}) \\ V_{BB,rm}(\omega_{rm}) &= \frac{\beta}{\gamma} V_{bl} \frac{R_L}{R_{sw}+R_L} H(\omega_{bl}+\omega_{LO}) \end{aligned} \tag{2.31}$$

Investigating the ratio between $V_{BB,rm,1}$ and $V_{BB,s,1}$, it seems that the reciprocal mixing has been reduced by the filtering effect of the lower phase. Without this effect, the ratio would be equal to β.

$$\frac{V_{BB,rm}(\omega_{rm})}{V_{BB,s}(\omega_s)} = \beta \frac{H(\omega_{bl})}{H(\omega_s+\omega_{LO})} \tag{2.32}$$

However, the lower branch also generates reciprocal mixing voltage on the RF node. Because this node is shared with the upper phase, this reciprocal mixing is mixed to the baseband of this phase, adding to the reciprocal mixing term.

$$V_{RF,rm}(\omega_{rm}) = \beta V_{bl} \left(H(\omega_{rm}) - H(\omega_{bl})\right) \tag{2.33}$$

$$\Delta V_{BB,rm}(\omega_{rm}) = \frac{R_L}{R_{sw}+R_L} \frac{V_{RF,rm}(\omega_{rm}+\omega_{LO})}{\gamma} \tag{2.34}$$

Adding this term to the original baseband reciprocal mixing term from equation 2.31 yields equation 2.35.

$$\begin{aligned} V_{BB,rm,t} &= V_{BB,rm} + \Delta V_{BB,rm}(\omega_{rm}) \\ &= \frac{\beta}{\gamma} V_{bl} \frac{R_L}{R_{sw}+R_L} H(\omega_{bl}+\omega_{LO}) + \frac{\beta}{\gamma} V_{bl} \frac{R_L}{R_{sw}+R_L} \left(H(\omega_{rm}+\omega_{LO}) - H(\omega_{bl}+\omega_{LO})\right) \\ &= \frac{\beta}{\gamma} V_{bl} \frac{R_L}{R_{sw}+R_L} H(\omega_{rm}+\omega_{LO}) \end{aligned} \tag{2.35}$$

This approach also does not work. Investigating the ratio between reciprocal mixing and wanted signal at baseband again, this time with the total reciprocal mixing term, shows that there is no improvement. The ratio is again β.

$$\frac{V_{BB,rm,t}(\omega_{rm})}{V_{BB,s}(\omega_s)} = \beta \frac{H(\omega_{rm}+\omega_{LO})}{H(\omega_s+\omega_{LO})} = \beta \tag{2.36}$$

The results are verified using simulation of this setup with N=4. The parameters are: β=1m, f_{LO}=1 GHz, R_S=50Ω, R_{sw}=5Ω, R_L=200Ω and C_L=100 pF. The baseband signals were summed such that the reciprocal mixing term is zero at 0 Hz. Figure 2.16 shows that not only the reciprocal mixing is cancelled, but the signal is also gone. Again, at baseband, the ratio between reciprocal mixing and wanted signal is equal to β for every frequency.

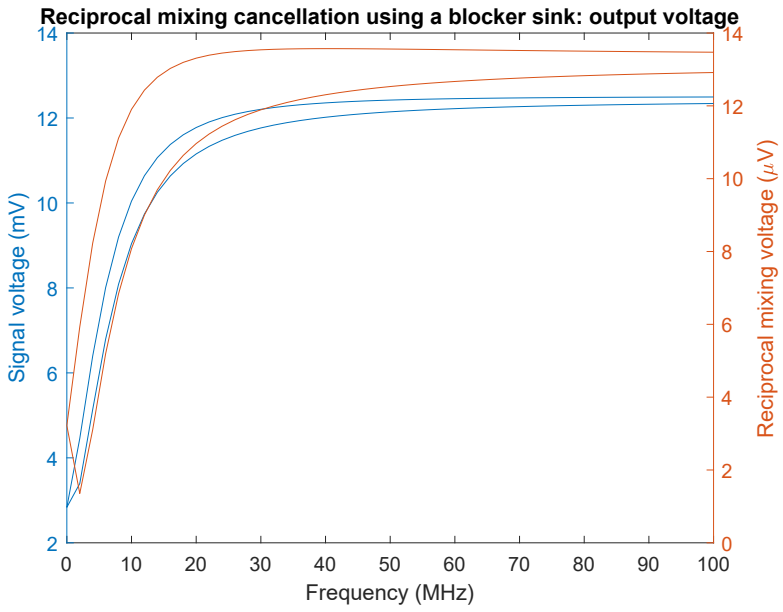

Figure 2.16: Simulation of reciprocal mixing cancellation idea 3

2.4.4. IDEA 4: IMAGE

The image of a signal spectrum is defined as the same spectrum mirrored around a certain frequency. If an image is made of spectrum around the LO frequency and this signal is downconverted, its reciprocal mixing has the opposite sign of the reciprocal mixing from the original downconverted signal. When the spectrum is mirrored around the LO, blockers that were above the LO frequency end up below the LO frequency (and vice versa), maintaining their relative frequency. For example, when a blocker at 800 MHz is mirrored around an LO of 1GHz, it ends up at 1.2 GHz. Since the blocker is now on the 'other side' of the LO, it mixes with the other sideband of the LO phase noise when downconverting. Since we know that the phase noise is symmetric around the LO, except 180 degrees out of phase, the reciprocal mixing is the same, but 180 degrees out of phase. Figure 2.17a shows this visually, representing the phase noise by spurs.

Having a path with the original spectrum and another path with the mirrored spectrum, it becomes possible to rotate the baseband signals from these paths and add them together, preserving the original signal while cancelling the reciprocal mixing. This process is shown in Figure 2.19. Figure 2.18 shows the circuit diagram of this idea.

To make this work, an image must be generated. A possibility is to use a double quadrature mixer. The first mixer downconverts the signal to baseband. The Q path is inverted, mirroring the spectrum around DC.

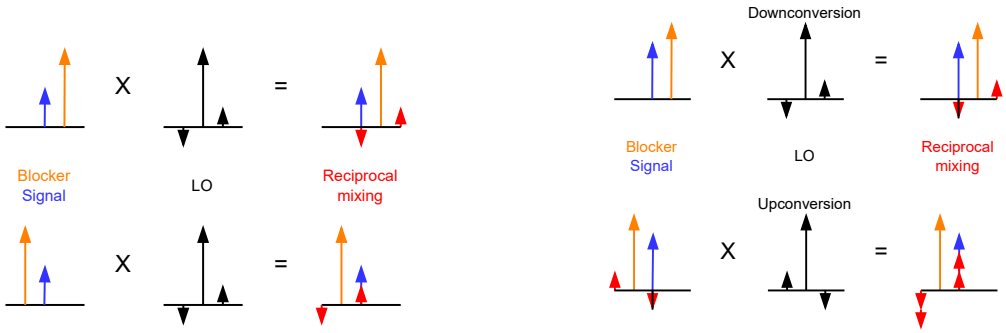

(a) Reciprocal mixing terms of a signal compared to its image

(b) Reciprocal mixing terms produced by image generation

Figure 2.17: Reciprocal mixing behaviour with a spectral image

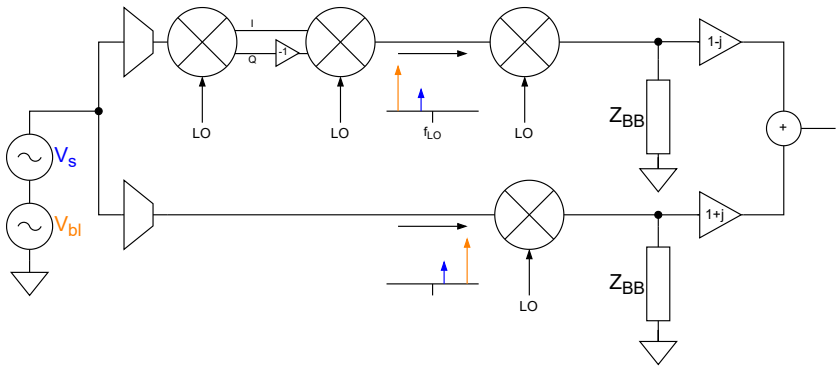

Figure 2.18: Reciprocal mixing cancellation using a spectral image

This mirrored signal is upconverted to RF by the second mixer. However, the LO driving these mixers also have phase noise and consequently creates reciprocal mixing. Including reciprocal mixing in the analysis, as done in Figure 2.17b, shows that the mirrored spectrum has reciprocal mixing at RF, twice the amount that it presents at baseband (relative to the signal amplitude). This reciprocal mixing term caused by the image generation effectively inverts the phase of the reciprocal mixing of the image spectrum converted to baseband, as it is twice the amplitude and opposite phase of the reciprocal mixing term caused by the downconversion to baseband. In the end, the amplitude of reciprocal mixing term remains the same.

This conclusion is verified using simulation of this setup using 4-path mixers. The parameters are: β=1m, f_{LO}=1 GHz, R_S=50Ω, R_{sw}=5Ω, R_L=200Ω and C_L=100 pF. Figure 2.20a shows both input signals. The first has the original signal and the other the image. Also, the second path has a reciprocal mixing term. After down-

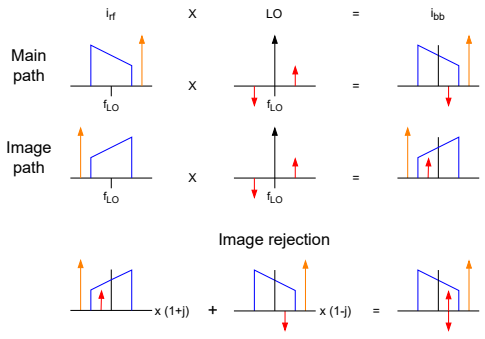

Figure 2.19: Reciprocal mixing cancellation with image rejection

conversion to baseband the signals look the same. Investigating the phase shows that for both paths, the reciprocal mixing is in phase with the wanted signal, supporting the conclusion that it is not possible to cancel reciprocal mixing using this method.

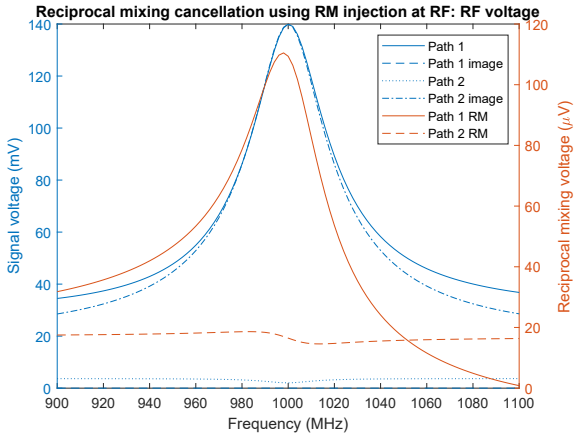

(a) RF signals

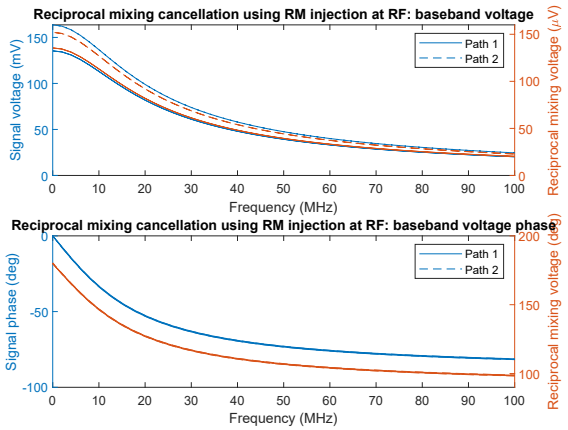

(b) Baseband signals

Figure 2.20: Simulation of reciprocal mixing cancellation idea 4

2.5. CONCLUSION

This research indicates that is is impossible to cancel reciprocal mixing with just linear components: gain, transconductance, mixers and baseband filters. Since the mixers and filters are linear, the relation between reciprocal mixing and blocker power is fixed, only dependent on the LO phase noise. To support this claim, the equations for the signal, blocker and reciprocal mixing voltage on both the RF and BB nodes of an N-path filter are summarized as input voltages multiplied by transfer functions. The transfer function is defined in equation 2.37.

$$H(\omega) = \frac{R_{sw} + Z_{RF}(\omega)}{R_S + R_{sw} + Z_{RF}(\omega)} \tag{2.37}$$

$$\begin{aligned} V_{RF,s} &= V_s H(\omega_s) \\ V_{RF,bl} &= V_{bl} H(\omega_{bl}) \\ V_{RF,rm} &= \beta V_{bl} \left(H(\omega_s) - H(\omega_{bl})\right) \\ &= \beta \left(\frac{V_{bl}}{V_s} V_{RF,s} - V_{RF,bl} \right) \end{aligned} \tag{2.38}$$

These equations show that the only way to make $V_{RF,rm}$ zero is when $H(\omega_s) = H(\omega_{bl})$. But this means there is no filtering, since the transfer function of signal and blocker are the same. To show that this holds for any circuit made with N-path filters and frequency-independent linear components, it is noted that this network can be represented by scaling factors. An arbitrarily complicated network of many N-path filters can therefore be modeled by matrix equation 2.39.

$$\begin{bmatrix} V_s H_0(\omega_s) & \cdots & V_s H_m(\omega_s) \\ V_{bl} H_0(\omega_{bl}) & \cdots & V_{bl} H_m(\omega_{bl}) \\ \beta V_{bl} \left(H_0(\omega_s) - H_0(\omega_{bl})\right) & \cdots & \beta V_{bl} \left(H_m(\omega_s) - H_m(\omega_{bl})\right) \end{bmatrix} \begin{bmatrix} A_0 \\ \vdots \\ A_m \end{bmatrix} = \begin{bmatrix} V_{RF,s} \\ V_{RF,bl} \\ V_{RF,rm} \end{bmatrix} \tag{2.39}$$

Let's define a new transfer function, which is a weighted sum of the transfer functions of all the filters.

$$H_t(\omega) = \sum_{k=0}^{m} A_m H_m(\omega) \tag{2.40}$$

The matrix equation can be rewritten using this definition. The result, shown in equation 2.41, is the same as in equation 2.38. Again, the only possibility to cancel reciprocal mixing is when there is no filtering. This proves it is not possible to cancel reciprocal mixing at the RF side using linear frequency-independent components.

$$\begin{aligned} V_{RF,s} &= V_s H_t(\omega_s) \\ V_{RF,bl} &= V_{bl} H_t(\omega_{bl}) \\ V_{RF,rm} &= \beta V_{bl} \left(H_t(\omega_s) - H_t(\omega_{bl})\right) \\ &= \frac{V_{bl}}{V_s} V_{RF,s} - V_{RF,bl} \end{aligned} \tag{2.41}$$

For the baseband signals, the same transfer function can be used as with the RF signals. Only an transfer function from RF to baseband is needed. This is defined in equation 2.42. Using this equation, the signals at baseband are represented by input voltages multiplied by transfer functions, as shown in equation 2.43.

$$H_{BB}(\omega) = \frac{\gamma}{N} \frac{Z_B(\omega)}{R_{sw} + Z_{RF}(\omega)} \tag{2.42}$$

$$\begin{aligned} V_{BB,s} &= V_s H_{BB}(\omega_s) H(\omega_s + \omega_{LO}) \\ V_{BB,bl} &= V_{bl} H_{BB}(\omega_{bl}) H(\omega_{bl} + \omega_{LO}) \\ V_{RF,rm} &= \beta V_{bl} H_{BB}(\omega_s) H(\omega_s + \omega_{LO}) \end{aligned} \tag{2.43}$$

There are two ways in this equation to have zero reciprocal mixing: either $H_{BB}(\omega_s)$ is zero or $H(\omega_s + \omega_{LO})$. Both have the result that the wanted signal $V_{BB,s}$ is also zero. This also holds for any network of N-path filters with linear components, since such a network can be represented by a (frequency-dependent) scaling factor. The frequency dependence does not have any meaningful effect that can be used for reciprocal mixing cancellation, because the wanted signal and reciprocal mixing are at the same frequency.

It is, obviously, possible to cancel reciprocal mixing when filtering at RF is done without using N-path filters. Doing this, the advantages of having an N-path filter are lost: the filter center frequency is no longer adjustable. Also, if some device exists that can generate an image of the signal without using mixers, it is possible to cancel out reciprocal mixing. It is unlikely that this device exists, because image generation is essentially a mixing operation.

Therefore this research must conclude that it is not possible to cancel reciprocal mixing in N-path filters using linear components. It may well be possible with non-linear components. Prior research [6] shows that it is possible using a PLL that tracks the blocker. Other methods for reciprocal mixing cancellation using other non-linear components could be possible.

3

N-PATH INHERENT NON-LINEARITY

In the drive towards higher data speeds and with the increase of the number of connected devices, the available spectrum needs to be used efficiently. Receivers can expect blockers, both close in and far out-of-band. This places stringent requirements on the linearity of the receiver. If an N-path filter is to be used, this filter also needs to meet these requirement. Because N-path filters use NMOS transistors in a passive way, they are inherently very linear. The goal of this research is to analyse what factors contribute to linearity, and to use this knowledge to design a highly linear receiver with an N-path filter.

3.1. PRIOR ART

N-path based receivers generally report high linearity. Table 3.1 shows some designs with out-of-band input third order intercept point (IIP3) ranging from 11 to 28 dBm. Papers generally attribute this high linearity to a property of the passive mixer. N-path filters can also be seen as passive mixers connected to baseband impedances. Assuming the baseband impedances (resistors and capacitors) are intrinsically linear, the source of distortion is the mixer. Khatri et al.[7] analysed the distortion in passive mixers using Volterra series. These results are useful for the analysis of an N-path filter, but cannot be directly applied because of the influence of the frequency-dependent impedance. Also, an N-path notch filter usually has two switches in series, which complicates the analysis.

	Elmi et al.[10]	Lin et al.[11]	Huang et al.[5]	Soer et al.[3]	Andrews et al.[4]
RF input	single ended	single ended	single ended	differential	single ended
N	8	8	8	4	8
Freq. range (GHz)	0.1 - 2	0.15 - 0.85	3.7 - 6.5	0.2 - 2.0	0.1-2.4
DSB NF (dB)	<4	4.6 ± 0.9	2.4-4.7	6.5	4 ± 1
S11 (dB)	<-10	-12			-30
OOB-IIP3 (dBm)	15.9	17.4	28	11	25
Bandwidth (MHz)	1	9		25	20
Supply (V)	1.2	1.2 / 2.5		1.2	1.2 / 2.5
CMOS technology	90nm	65nm	45nm SOI	65nm	65nm

Table 3.1: Comparison of some N-path receivers from recent literature

3.2. METHOD

The intermodulation distortion of N-path filters, both bandpass and notch, is analysed and modeled. This model is verified using simulation. Using these N-path filters, three receiver architectures are proposed and their linearity compared, using the insight from the analysis of the N-path filter. The architectures are compared on IIP3 and OIP3, for both in- and out-of-band blockers.

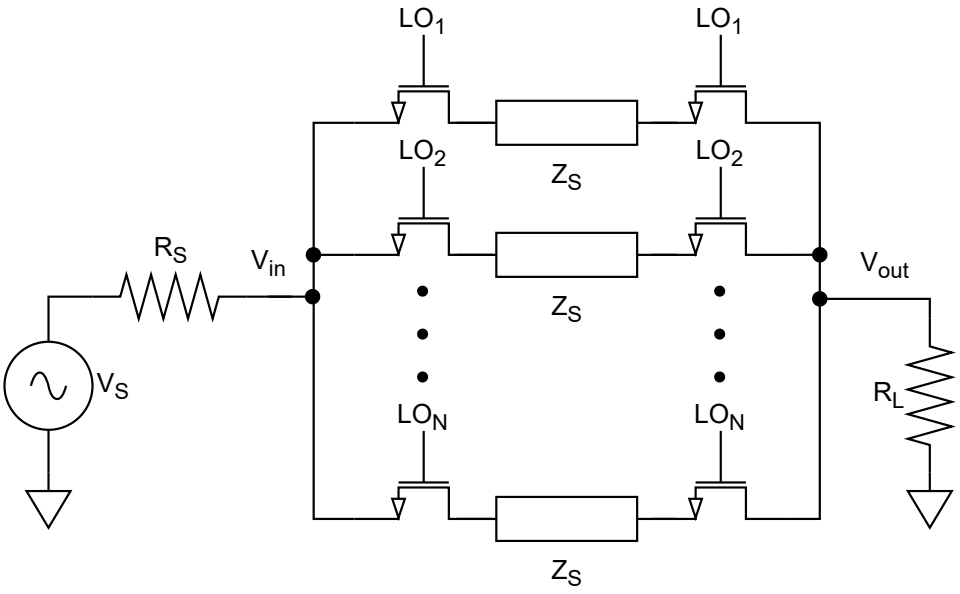

Figure 3.1: An N-path notch filter.

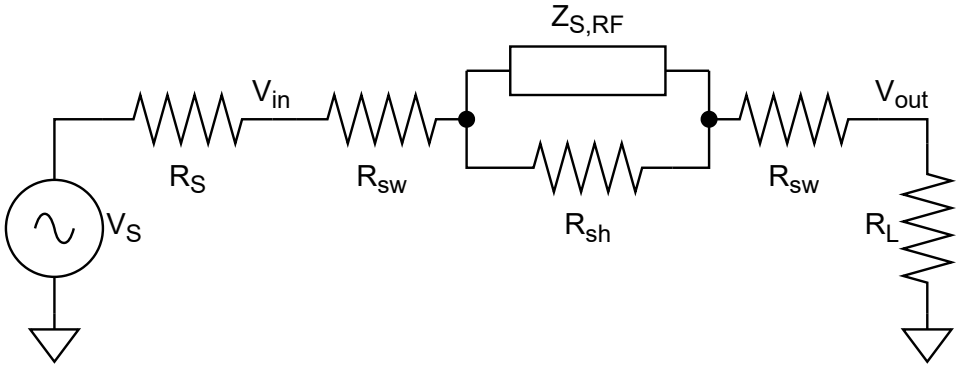

Figure 3.2: Simplified model for analysis of an N-path notch filter.

3.3. THEORY

In an N-path filter, the N-MOS switches are either in an off state or in the linear region. The non-linearity of the switch in the off state does not need to be taken into consideration, since there is no significant current going trough the switch. In the saturation state, there are several sources of non-linearity to consider: modulation of the on-resistance, and non-linear input and output capacitance. The effects of these non-linearity sources on the filter linearity scale differently with switch size. Furthermore, the switch size also influences the linear transfer of the filter. Models are derived for the IM3 caused by R_{on} modulation in N-path filters, both notch and bandpass type. These models are compared against simulation results.

3.3.1. IM3 MODEL

Obtaining a model of the IM3 generated in an N-path filter starts with a linear model of the signal transfer. In section 2.2.1 a model was derived for the bandpass N-path filter, which can be used as the basis for the IM3 model. For the notch filter, the model has to be adapted.

An N-path notch filter has a switched impedance in series with the input and terminated with a load impedance. Figure 3.1 shows such a filter. The series impedance Z_S is typically just a capacitor. Just as in the bandpass

case, it is possible to replace the switched impedances with a single RF equivalent impedance. Figure 3.2 shows the result. Again there is a shunt resistor modeling the switching loss, which depends on the source and load impedance and the switch on-resistance. The formula for the equivalent impedance is the same as for the bandpass filter, but it is mentioned for completeness in equation 3.2.

$$\begin{aligned} R_{sh,BB} &= \frac{N}{1-\gamma^2}(R_S + R_L + 2R_{sw}) \\ R_{sh,RF} &= \frac{\gamma^2}{N} R_{sh,BB} = \frac{\gamma^2}{1-\gamma^2}(R_S + R_L + 2R_{sw}) \end{aligned} \tag{3.1}$$

$$\begin{aligned} Z_{S,RF}(\omega) &= \frac{\gamma^2}{N} Z_S(\omega - \omega_{LO}) \\ Z_{BB}(\omega) &= \frac{R_{sh,BB} Z_S(\omega)}{R_{sh,BB} + Z_S(\omega)} \\ Z_{RF}(\omega) &= \frac{\gamma^2}{N} Z_{BB}(\omega - \omega_{LO}) = \frac{Z_{S,RF}(\omega) R_{sh,RF}}{Z_S(\omega) + R_{sh,RF}} \end{aligned} \tag{3.2}$$

Knowing the expression for Z_{RF} and the topology of the circuit, the expressions for the RF current can be derived. With this expression, the input and output voltages are calculated. The result is shown in equations 3.4 and 3.5.

$$I_{RF}(\omega) = \frac{V_S}{R_S + R_L + 2R_{sw} + Z_{RF}(\omega)} \tag{3.3}$$

$$V_{in,RF}(\omega) = V_S - R_S I_{RF}(\omega) = V_S \frac{R_L + 2R_{sw} + Z_{RF}(\omega)}{R_S + R_L + 2R_{sw} + Z_{RF}(\omega)} \tag{3.4}$$

$$V_{out,RF}(\omega) = R_L I_{RF}(\omega) = V_S \frac{R_L}{R_S + R_L + 2R_{sw} + Z_{RF}(\omega)} \tag{3.5}$$

As before, a simplified model can be derived for the N-path filter. Figure 3.3 shows the simplification for a bandpass N-path filter, with the non-linearity of the transistor on-resistance taken into account. The contributions of all the transistors can be combined into one non-linear element. This is because the transistors do not influence any signals when they are switched off. This process can be repeated for the N-path notch filter, expanding the linear model by adding a non-linear current source which is dependent on the transistors drain-source voltage.

Third order linearity is usually measured with a two tone test. In such a test, two tones are presented to the device, and their mixing products measured. This analysis follows the same procedure to predict IM3 in an N-path filter. The two tones are at $f_1 = f_c + \Delta f$ and $f_2 = f_c + \Delta f - f_{off}$ in which f_c is chosen to be the filter center frequency. This will produce a third order harmonic at $f_{IM3} = 2f_1 - f_2 = f_c + f_{off}$. The filter bandwidth and f_{off} are chosen such that this IM3 tone is in the filter bandwidth. There are also other third order harmonics, but they are outside the filter bandwidth and therefore not important for this analysis.

For this analysis, R_{sh} is absorbed in Z_{RF}. If the number of phases is large (e.g. N≥8), the effects of R_{sh} are very small and can be ignored.

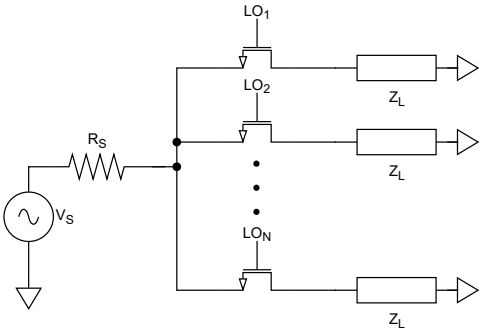

(a) N-path band pass filter

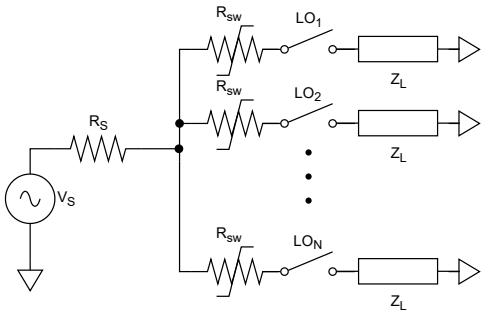

(b) N-path band pass filter with transistors modeled as non-linear conductances and ideal switches

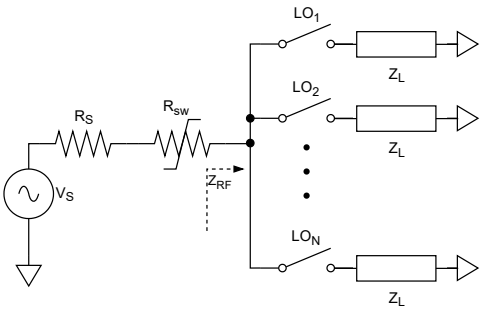

(c) Simplified model for nonoverlapping LO phases

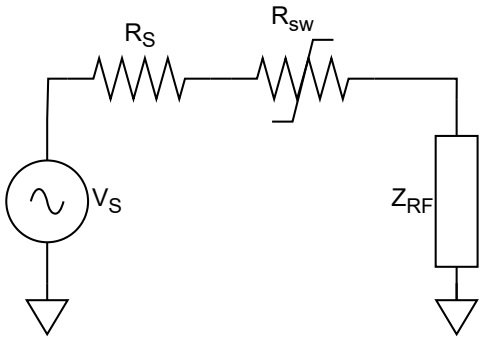

(d) Single-phase equivalent

Figure 3.3: Derivation of a simplified schematic for non-linear analysis of the N-path band pass filter.

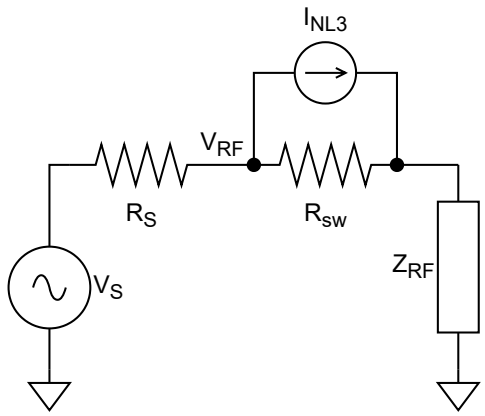

Figure 3.4: Circuit for non-linear analysis of N-path band pass filter

BAND PASS FILTER

Figure 3.4 shows the circuit used for the non-linear analysis. The non-linear conductance is modeled by a resistor, parallel with a dependent current source. The resistor models the linear part of the switch, the switch on-resistance.

The gate-source voltage of the transistor is the same as V_{RF} from equation 2.5, only negative.

$$V_{GS}(\omega) = -V_{RF}(\omega) \tag{3.6}$$

The non-linear current source is a third order product of the transistor gate-source voltage. Equation 3.7 shows that the non-linear current is dependent on the first tone to the second order multiplied by the second tone. This gives the IM3 tone of interest, which is equal to twice the first tone frequency minus the second tone frequency.

$$I_{NL3}(\omega_{IM3}) = g_3 V_{GS}(\omega_1)^2 V_{GS}(\omega_2) \tag{3.7}$$

A part of this current flows through the switch itself, while a the rest flows through the rest of the circuit. Equation 3.8 gives this part of the current, which produces a third order voltage on all the circuit nodes. The voltage on the filter input node is given by equation 3.9.

$$I_{RF3}(\omega_{IM3}) = I_{NL3}(\omega_{IM3}) \frac{R_{sw}}{R_S + R_{sw} + Z_{RF}(\omega_{IM3})} \tag{3.8}$$

$$\begin{aligned} V_{RF3}(\omega_{IM3}) =& - I_{RF,3}(\omega_{IM3}) R_S \\ =& g_3 R_S V_S^3 \frac{(R_{sw} + Z_{RF}(\omega_1))^2}{(R_S + R_{sw} + Z_{RF}(\omega_1))^2} \frac{R_{sw} + Z_{RF}(\omega_2)}{R_S + R_{sw} + Z_{RF}(\omega_2)} \frac{R_{sw}}{R_S + R_{sw} + Z_{RF}(\omega_{IM3})} \end{aligned} \tag{3.9}$$

Knowing all the voltages and currents, the signal and IM3 powers can be calculated. From these, the IIP3 is derived, as shown in equation 3.12. Since this circuit has only one node, the IIP3 and OIP3 are the same.

$$P_{sig}(\omega_1) = V_{RF}(\omega_1) I_{RF}(\omega_1) = V_S^2 \frac{R_{sw} + Z_{RF}(\omega_1)}{(R_S + R_{sw} + Z_{RF}(\omega_1))^2} \tag{3.10}$$

$$P_{IM3}(\omega_{IM3}) = -I_{RF,3}(\omega_{IM3}) V_{RF3}(\omega_{IM3}) = I_{RF,3}(\omega_{IM3})^2 R_S \tag{3.11}$$

$$\begin{aligned} IIP3 =& 10 \log_{10} \sqrt{\frac{P_{sig}(\omega_1)^3}{P_{IM3}(\omega_{IM3})}} \\ =& 10 \log_{10} \left(\frac{(R_{sw} + Z_{RF}(\omega_2))(R_S + R_{sw} + Z_{RF}(\omega_{IM3}))}{g_3 \sqrt{R_S} R_{sw} \sqrt{R_{sw} + Z_{RF}(\omega_1)} (R_S + R_{sw} + Z_{RF}(\omega_1))(R_{sw} + Z_{RF}(\omega_2))} \right) \end{aligned} \tag{3.12}$$

NOTCH FILTER

For the notch filter, the same process as with the band pass filter is conducted, resulting in the circuit in figure 3.5. Again, the starting point of the analysis is the RF voltage, as given by equation 3.4. The drain-source voltage and the resulting non-linear current for both transistors is shown in equations 3.13 and 3.14.

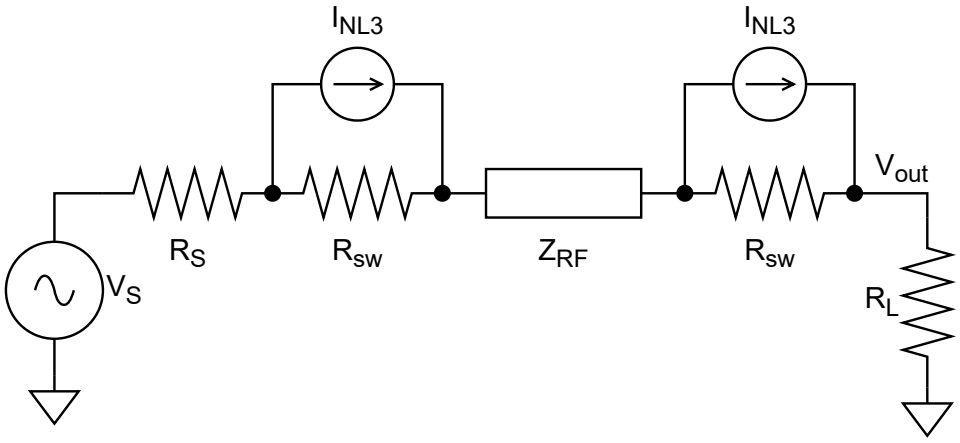

Figure 3.5: Circuit for non-linear analysis of N-path notch filter

$$\begin{aligned} V_{GS,1}(\omega) &= -V_{in,RF}(\omega) \\ V_{GS,2}(\omega) &= -(R_{sw}+R_L)I_{RF}(\omega) \end{aligned} \tag{3.13}$$

$$\begin{aligned} I_{NL3,1}(\omega_{IM3}) &= g_3 V_{GS,1}(\omega_1)^2 V_{GS,1}(\omega_2) \\ I_{NL3,2}(\omega_{IM3}) &= g_3 V_{GS,2}(\omega_1)^2 V_{GS,2}(\omega_2) \end{aligned} \tag{3.14}$$

To find the IM3 at the input and output of the filter, the non-linear current flowing through these impedances must be know. The notch filter has two non-linear current sources, and their contribution to the non-linear current flowing through R_L and R_S is the same. Equation 3.15 gives the total non-linear current, which produces a third order voltage on all the circuit nodes. The voltage on the filter input node is given by equation 3.16.

$$I_{RF3}(\omega_{IM3}) = (I_{NL3,1}(\omega_{IM3}) + I_{NL3,2}(\omega_{IM3}))\frac{R_{sw}}{R_S+R_L+2R_{sw}+Z_{RF}(\omega_{IM3})} \tag{3.15}$$

$$\begin{aligned} V_{in,RF3}(\omega_{IM3}) &= -I_{RF,3}(\omega_{IM3})R_S \\ V_{out,RF3}(\omega_{IM3}) &= I_{RF,3}(\omega_{IM3})R_S \end{aligned} \tag{3.16}$$

Knowing all the voltages and currents, the signal and IM3 powers at the input and output node can be calculated. From these, the OIP3 and IIP3 are derived. In contrast to the bandpass filter, the notch filter has a distinct input and output nodes, and thus the OIP3 and IIP3 are different. They are expressed in equation 3.19.

$$\begin{aligned} P_{in,sig}(\omega_1) &= V_{in,RF}(\omega_1)I_{RF}(\omega_1) = V_S^2\frac{R_L+2R_{sw}+Z_{RF}(\omega_1)}{(R_S+2R_{sw}+Z_{RF}(\omega_1))^2} \\ P_{out,sig}(\omega_1) &= V_{out,RF}(\omega_1)I_{RF}(\omega_1) = V_S^2\frac{R_L}{(R_S+2R_{sw}+Z_{RF}(\omega_1))^2} \end{aligned} \tag{3.17}$$

$$\begin{aligned} P_{in,IM3}(\omega_{IM3}) &= -I_{RF,3}(\omega_{IM3})V_{in,RF3}(\omega_{IM3}) = I_{RF,3}(\omega_{IM3})^2 R_S \\ P_{out,IM3}(\omega_{IM3}) &= I_{RF,3}(\omega_{IM3})V_{out,RF3}(\omega_{IM3}) = I_{RF,3}(\omega_{IM3})^2 R_L \end{aligned} \tag{3.18}$$

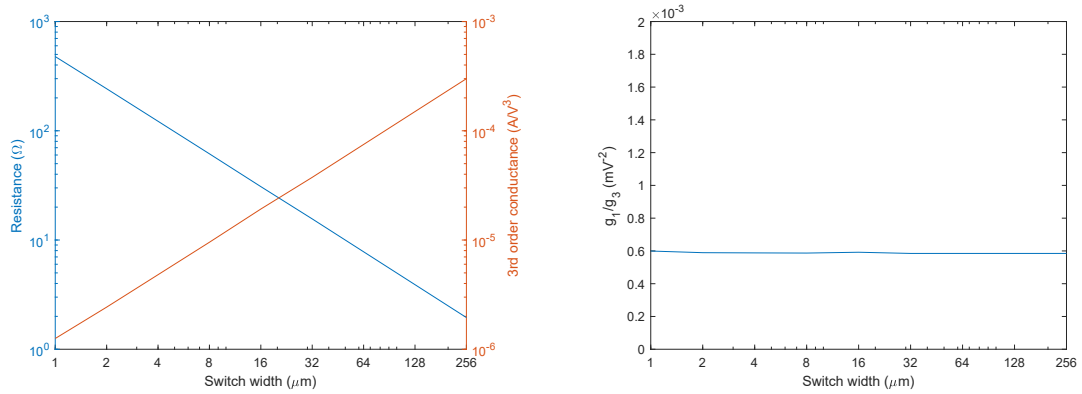

(a) NMOS on-resistance and third order conductance versus transistor width.(b) Ratio between first and third order conductance versus transistor width.

Figure 3.6: NMOS linearity when used as a switch

$$
\begin{aligned}
IIP3 =& 10\log_{10}\sqrt{\frac{P_{out,sig}(\omega_1)P_{in,sig}(\omega_1)^2}{P_{out,IM3}(\omega_{IM3})}} \\
=& 10\log_{10}\left(\frac{(R_L+2R_{sw}+Z_{RF}(\omega_1))(R_S+R_L+2R_{sw}+Z_{RF}(\omega_2))(R_S+R_L+2R_{sw}+Z_{RF}(\omega_{IM3}))}{g_3R_{sw}\left((R_L+2R_{sw}+Z_{RF}(\omega_1))^2(R_L+2R_{sw}+Z_{RF}(\omega_2))+(R_L+R_{sw})^3\right)(R_S+R_L+2R_{sw}+Z_{RF}(\omega_1))}\right) \\
OIP3 =& 10\log_{10}\sqrt{\frac{P_{out,sig}(\omega_1)^2}{P_{out,IM3}(\omega_{IM3})}} \\
=& 10\log_{10}\left(\frac{(R_L+2R_{sw}+Z_{RF}(\omega_1))^2(R_S+R_L+2R_{sw}+Z_{RF}(\omega_2))(R_S+R_L+2R_{sw}+Z_{RF}(\omega_{IM3}))}{g_3R_LR_{sw}\left((R_L+2R_{sw}+Z_{RF}(\omega_1))^2(R_L+2R_{sw}+Z_{RF}(\omega_2))+(R_L+R_{sw})^3\right)(R_S+R_L+2R_{sw}+Z_{RF}(\omega_1))}\right)
\end{aligned}
\tag{3.19}
$$

3.3.2. MODEL VERIFICATION

Values for R_{sw} and g_3 are extracted from pss simulation of a single transistor. V_{GS} is biased at 1 Volt DC. A small (50 mV) low frequency sinusoidal voltage (10 MHz) is used to drive V_S while the resulting drain current is measured. The first- and third-order components are measured for a range of transistor widths. Figure 3.6a shows the results, plotted as a log-log plot. R_{sw} is inversely proportional to the transistor width, while g_3 scales proportional to the transistor width. This means the ratio between first- and third order conductance $\frac{g_1}{g_3}$), which is equal to the product of R_{sw} and g_3 is almost constant (Figure 3.6b). Thus, the scaling of the transistor does not influence the linearity of a single transistor when used as a switch. However, the derived expressions for IIP3 and OIP3 depend linearly on g_3 and on higher orders of Rsw, so their combined effects on the linearity of an N-path filter do not cancel out.

The fact that the product of R_{sw} and g_3 is constant can be applied to the IP3 equations, equation and equation 3.19, by replacing $R_{sw}\cdot g_3$ with k_3. R_{sw} can be modeled by a resistivity divided by the switch width ($R_{sw}=\frac{\rho}{W}$). The resulting equations are and 3.21. The values for these constants are obtained by taking the average over all measurements. The value of the resistivity is $499\Omega\cdot\mu m$ and the value of k_3 is $4.16\cdot10^{-}4V^{-2}$.

$$
IIP3_{bpf} = 10\log_{10}\left(\frac{\sqrt{\frac{\rho}{W}+Z_{L,RF}(\omega_1)}^3\left(R_S+\frac{\rho}{W}+Z_{L,RF}(\omega_2)\right)\left(R_S+\frac{\rho}{W}+Z_{L,RF}(\omega_{IM3})\right)}{k_3\sqrt{R_S}\left(\frac{\rho}{W}\right)^3\left(R_S+\frac{\rho}{W}+Z_{L,RF}(\omega_1)\right)}\right) \tag{3.20}
$$

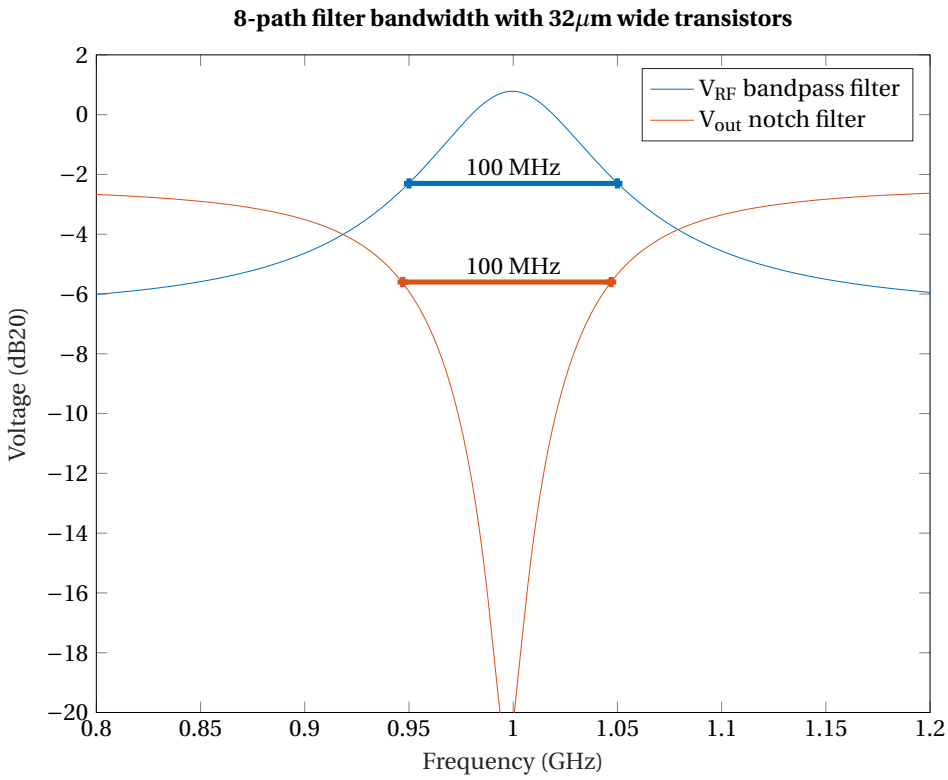

Figure 3.7: Bandwidth of the measured 8-path filters

$$
\begin{aligned}
IIP3_{notch} &= 10\log_{10}\left(\frac{\left(R_L+2\frac{\rho}{W}+Z_{RF}(\omega_1)\right)\left(R_S+R_L+2\frac{\rho}{W}+Z_{RF}(\omega_2)\right)\left(R_S+R_L+2\frac{\rho}{W}+Z_{RF}(\omega_{IM3})\right)}{2k_3\left(\frac{\rho}{W}\right)^3\left(R_S+R_L+2\frac{\rho}{W}+Z_{RF}(\omega_1)\right)}\right) \\
OIP3_{notch} &= 10\log_{10}\left(\frac{R_L\left(R_S+R_L+2\frac{\rho}{W}+Z_{RF}(\omega_2)\right)\left(R_S+R_L+2\frac{\rho}{W}+Z_{RF}(\omega_{IM3})\right)}{2k_3\left(\frac{\rho}{W}\right)^3\left(R_S+R_L+2\frac{\rho}{W}+Z_{RF}(\omega_1)\right)}\right)
\end{aligned}
\tag{3.21}
$$

The notch and bandpass 8-path filters are simulated with different switch widths for an out-of-band blocker scenario. The input tones are at 1200 and 1402 MHz. All RF impedances are 50 Ω and the bandpass load impedance is $N\times 50 = 200\Omega$, so the filter is matched when the switch resistance is negligible. The capacitance for both filters is chosen such that thee -3dB bandwidth is 100 MHz for a switch width of $32\mu m$, as shown in figure 3.7. The IIP3 and OIP3 from the simulation results are compared to the model in Figures 3.8b and 3.9b.

Figure 3.8b shows the model prediction of the out-of-band linearity of the bandpass filter together with the simulation results. For small transistors, the transistor on resistance is much larger than the source and load impedances and thus it dominates the behaviour. The signal amplitude scales with R_{sw} and the IM3 tone scales with the signal amplitude and g_3, which also scales with the switch width. This results in an 10dB/decade slope for the signal power versus switch width and an 20dB/decade slope for the IM3 power versus switch width. IIP3 is calculated as $1.5\cdot P_{sig} - 0.5\cdot P_{IM3}$ when the powers are in dB scale. Combining the slopes with this formula results in the 5dB/decade IIP3 versus switch width slope which can be seen in Figure 3.8b. The simulation matches the model very well for small transistor widths (<8 μm).

For wide transistors, R_{sw} becomes small and insignificant compared to the other impedances in the circuit. The signal power is no longer dependent on the switch width. The IM3 current generated is dependent on g_3 and thus on the switch width, but because R_{sw} is small, this current is shunted by the transistor on resistance, negating the dependence on switch width. Figure 3.8b shows that the model expects that the IIP3 is constant for wide transistors. The transition point between dependence on R_{sw} and constant IIP3 depends

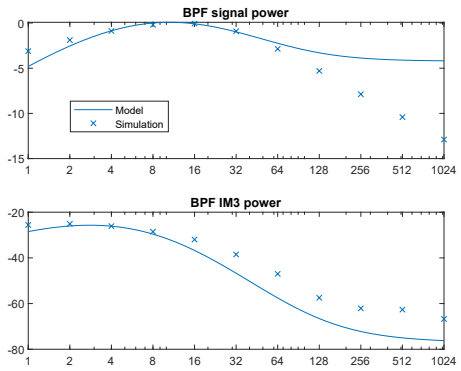

(a) Signal and IM3 power for N-path bandpass filter linearity calculations

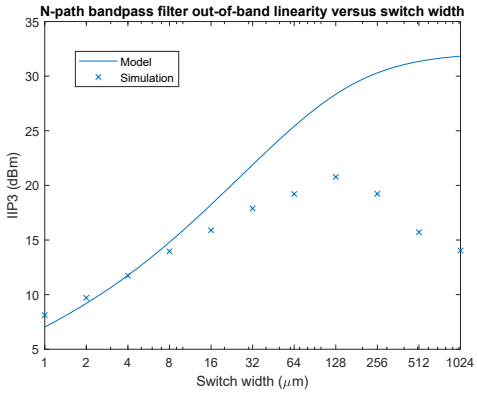

(b) N-path bandpass filter linearity versus switch width

Figure 3.8: N-path bandpass filter out-of-band linearity

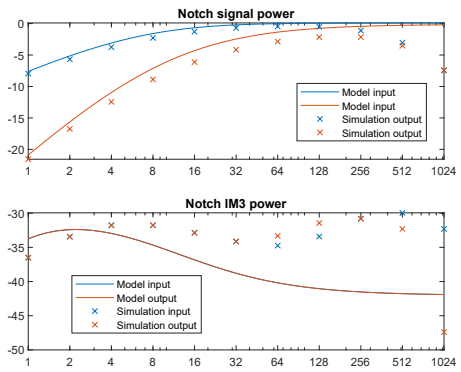

(a) Signal and IM3 power for N-path notch filter linearity calculations

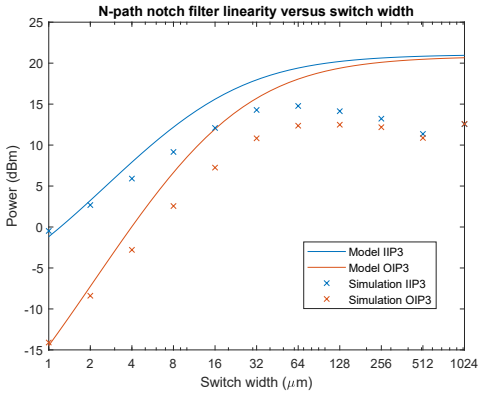

(b) N-path notch filter linearity versus switch width

Figure 3.9: N-path notch filter out-of-band linearity

on the impedance seen by the input tones. The model matches the general trend of the simulation results up until <128 μm. The simulation results show that for very wide transistors, the linearity actually degrades. This could be the result of other non-linear effects that the model does not account for, such as non-linear capacitance. For out-of-band signals, this impedance is determined by the capacitance and thus quite low. The transistor needs to be very wide to have a situation were its on-resistance does not dominate the filter behaviour. Therefore, the model predicts that the maximum attainable IIP3 is higher for signals that are further out-of-band.

Figure 3.8b shows the model prediction of the out-of-band linearity of the notch filter together with the simulation results. For small transistors, the situation is the same as for the bandpass filter: R_{sw} dominates the behaviour. The input power scales with 10dB/decade with respect to the switch width. Because the signal loss is also dependent on R_{sw}, the output power has a 20dB/decade slope with respect to the switch width. This results in a 5dB/decade IIP3 and a 10 dB/decade OIP3 versus switch width slope which can be seen in Figure 3.9b.

Increasing the transistor width diminishes the influence of R_{sw} on the circuit behavior until it becomes insignificant. For very wide transistors, the out-of-band signal loss is negligible, which means that the IIP3 is equal to the OIP3. In this situation, the signal power is determined only by the source and load impedance and is not dependent on the switch width. The switched capacitance presents a very low impedance to the out-of-band signals and does not influence these signals very much. As a consequence, the IIP3 and OIP3 do not depend on the signal frequency as long as the signals are out-of-band.

The model predicts the out-of-band IIP3 for small transistor widths ($\leq 32\mu m$) accurately. For larger transis-

tors the model deviates significantly. This can be explained by considering the influence of non-linear input and output capacitance of the NMOS switch. The model does not account for these. This capacitance, and thus the influence it has on the filter behaviour, increases with transistor width.

Knowing that the developed model accurately predicts the out-of-band linearity of smaller transistors, the model can be simplified for these scenarios. The only frequency-dependent variable is Z_{RF}, which is a low-pass impedance. For out-of-band frequencies, Z_{RF} is zero. In case of the bandpass filter, for in-band frequencies, Z_{RF} is equal to the RF equivalent of the load resistance. In case of the notch filter, Z_{RF} would be very large if the IM3 tone is very close to the filter center frequency. In reality, the IM3 tone is offset from the center, and Z_{RF} at this frequency is mostly dependent on the filter capacitance. Its value is defined in equation 3.1. Equation 3.22 summarizes the substitutions that are made for the simplification.

$$\begin{aligned} Z_{RF}(\omega_{OOB}) &\simeq 0 \\ Z_{RF,bpf}(\omega_{IB}) &\simeq R_{L,RF} \\ Z_{RF,notch}(\omega_{IB}) &\simeq \frac{\gamma^2}{2j\pi NCf_{off}} \end{aligned} \tag{3.22}$$

$$\begin{aligned} IIP3_{bpf,OOB} &\simeq 10\log_{10}\left(\frac{R_S+\frac{\rho}{W}+R_{L,RF}}{k_3\sqrt{R_S}\sqrt{\frac{\rho}{W}}}\right) \\ IIP3_{notch,OOB} &\simeq 10\log_{10}\left(\frac{(R_L+2\frac{\rho}{W})\left(R_S+R_L+2\frac{\rho}{W}+\frac{\gamma^2}{2j\pi NCf_{off}}\right)}{2k_3\left(\frac{\rho}{W}\right)^3}\right) \\ OIP3_{notch,OOB} &\simeq 10\log_{10}\left(\frac{R_L\left(R_S+R_L+2\frac{\rho}{W}+\frac{\gamma^2}{2j\pi NCf_{off}}\right)}{2k_3\left(\frac{\rho}{W}\right)^3}\right) \end{aligned} \tag{3.23}$$

Another useful assumption is that the filter is matched. This means that $R_S = R_L = R_{L,RF}$. These can all be replaced by R_S.

$$\begin{aligned} IIP3_{bpf,OOB} &\simeq 10\log_{10}\left(\frac{2R_S+\frac{\rho}{W}}{k_3\sqrt{R_S}\sqrt{\frac{\rho}{W}}}\right) \\ IIP3_{notch,OOB} &\simeq 10\log_{10}\left(\frac{\left(R_S+2\frac{\rho}{W}\right)\left(2R_S+2\frac{\rho}{W}+\frac{\gamma^2}{2j\pi NCf_{off}}\right)}{2k_3\left(\frac{\rho}{W}\right)^3}\right) \\ OIP3_{notch,OOB} &\simeq 10\log_{10}\left(\frac{R_L\left(2R_S+2\frac{\rho}{W}+\frac{\gamma^2}{2j\pi NCf_{off}}\right)}{2k_3\left(\frac{\rho}{W}\right)^3}\right) \end{aligned} \tag{3.24}$$

The last step is to take only the terms with the lowest order dependence on the transistor width W. This represents the assumption that the transistors are small.

$$\begin{aligned} IIP3_{bpf,OOB} &\simeq 10\log_{10}\left(\frac{\sqrt{W}}{k_3\sqrt{\rho R_S}}\right) \\ IIP3_{notch,OOB} &\simeq 10\log_{10}\left(\frac{2W}{k_3 rho}\right) \\ OIP3_{notch,OOB} &\simeq 10\log_{10}\left(\frac{W^2 R_S}{k_3\rho^2}\right) \end{aligned} \tag{3.25}$$

From these simplifications it can be concluded that the out-of-band IIP3 of the bandpass filter improves with 5dBm per decade with respect to the switch width. The out-of band IIP3 of the notch filter improves with 10 dBm per decade and the OIP3 of this filter with 20 dBm per decade. This simplification is only valid for very small switch sizes ($\leq 8\mu m$). For other switch sizes that are well predicted by the full model, the simplified model in equation 3.24 can be used.

CONCLUSION

For small switch sizes (<32μm), 3rd order non-linearity can be well predicted by modeling R_{on} modulation. Increasing the switch width improves linearity up to the point that the on-resistance is no longer significantly influencing the circuit. The linearity can be improved by using higher terminating impedances. Notch filters are more linear than their corresponding bandpass filters, because they suppress in band signals, which is where the IM3 is generated.

3.4. ARCHITECTURE

There are several architectures possible for a receiver with an N-path filter. The simplest design is a mixer-first receiver with a band pass filter, shown in figure 3.10a. This has some drawbacks: the filter has to match the antenna, so the filter impedance cannot be freely chosen. To get decent attenuation, the filter needs large switches. If an LNTA is placed before the N-path filter, as in figure 3.10b, it can provide the matching. The output impedance of the LNTA is typically much higher than the antenna impedance, reducing the need for large switches in the N-path filter. Additionally, having an amplifier between the antenna and the N-path filter prevents LO signals from the filter from leaking to the antenna. A notch filter can be put in the feedback path of an amplifier to get a bandpass response. Figure 3.11a shows this architecture. The loading impedance can be freely chosen in this setup, but the input impedance must match the antenna. Another disadvantage is that the N-path filter is not isolated from the antenna. LO signals from the filter will leak to the antenna. A variation of this is the Band Pass Common Gate (BPCG) structure shown in figure 3.11b [12]. This architecture has isolating amplifiers between the input and notch filter, and between the filter and the feedback. Therefore it allows freedom in choosing the matching impedance of the filter. Also, the LO cannot leak directly to the antenna. It can, however leak trough amplifiers A_2 and the common gate stage to the input.

3.4.1. BANDPASS RECEIVER ARCHITECTURES

The receiver architectures behave differently in terms of linearity. The mixer-first receiver consists only of an N-path filter, and the receiver linearity is equal to the filter linearity. The LNTA-first receiver is a cascade of an amplifier and a filter. Because of this, the IIP3 can be calculated using a simple formula. This is done in equation 3.26. The equation shows that for significant gain, the filter IIP3 is dominant. This is to be expected, because the filter has to deal with a higher amplitude signal. Also, the blocker is presented to the amplifier unattenuated, which increases amplifier power consumption and can cause compression. The LTNA-first receiver is simulated with an functional transconductance block with a 3rd order non-linearity, while the N-path filter non-linearity is swept by changing the transistor width. The transistor width can be related to N-path linearity using the simulation data from Chapter 3.3.2. Figure 3.12 compares the model to this simulation, showing good correspondence of simulation with the model.

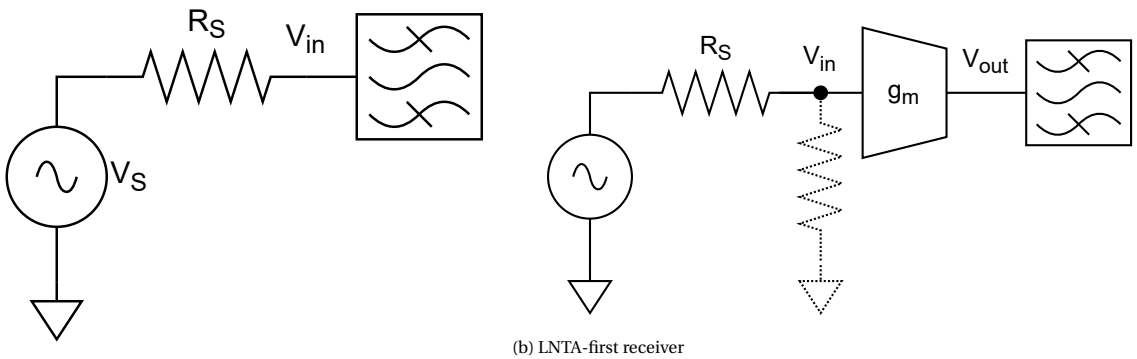

(a) Mixer-first receiver

(b) LNTA-first receiver

Figure 3.10: Receiver architectures with N-path bandpass filter

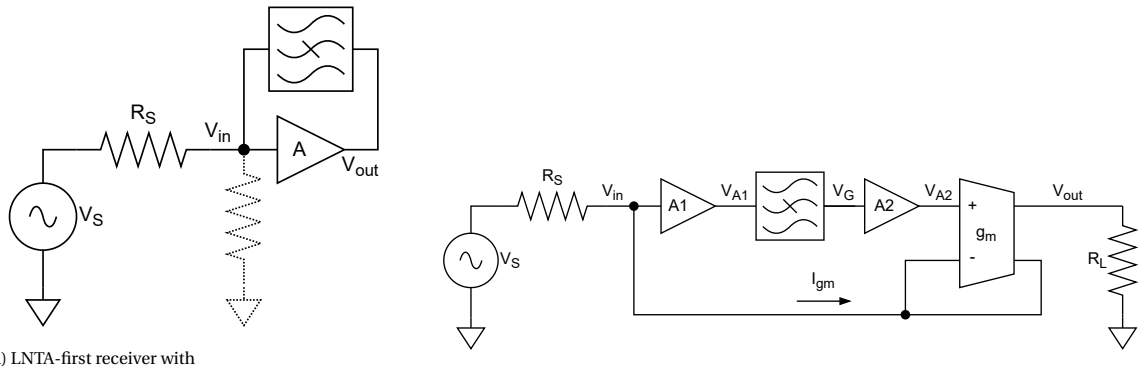

(a) LNTA-first receiver with filter in feedback path

(b) Bandpass common gate receiver

Figure 3.11: Receiver architectures with N-path notch filter

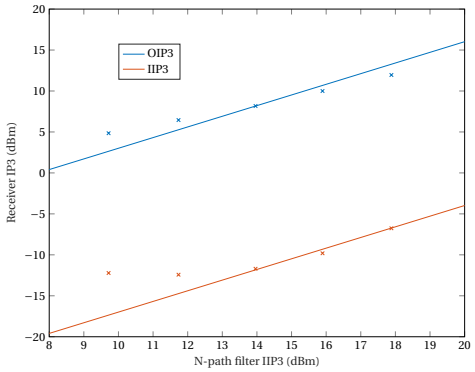

(a) Receiver linearity versus filter linearity. The amplifier is perfectly linear.

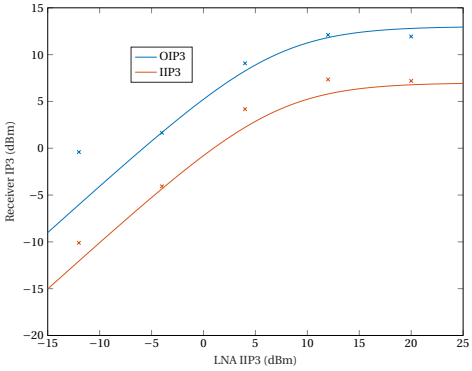

(b) Receiver linearity versus amplifier linearity. The N-path filter has 32μm wide switches, resulting in an IIP3 of 12 dBm.

Figure 3.12: Linearity of an LNTA-first receiver with bandpass N-path filter. The amplifier transconductance is 80 mS and the filter has an in-band impedance of 50 ohm, resulting in a voltage gain of 4.

$$IIP3_{rec} = \frac{1}{\frac{1}{IIP3_{LNTA}} + \frac{g_{m,LNTA} Z_{BPF}(f_{OOB})}{IIP3_{BPF}}} \tag{3.26}$$

3.4.2. LNA-FIRST RECEIVER WITH NOTCH FEEDBACK

The out-of-band third order linearity of the receiver with a notch in the feedback path is calculated. For this calculation it is assumed that the amplifier input is perfectly matched to the source. For simplicity, the filter is modeled as frequency-dependent voltage gain $G(f)$. The first order voltages are calculated with equations 3.27 and 3.28.

$$V_{in}(f) = \frac{1}{1 + AG(f)} V_S \tag{3.27}$$

$$V_{out}(f) = -\frac{A}{1 + AG(f)} V_S \tag{3.28}$$

The third order voltages are a function of the first order voltages. A_3 and G_3 are defined as the third order voltage gain of the amplifier and N-path filter respectively. Their values can be derived from the IIP3, as shown in equation 3.29.

$$\begin{aligned} A_3 &= \frac{A}{10^{\frac{IIP3_A}{10}}} \\ G_3(f) &= \frac{G(f)}{10^{\frac{IIP3_G}{10}}} \end{aligned} \tag{3.29}$$

Solving the node equations (eq. 3.30 for the output node yields equation 3.31.

$$\begin{aligned} V_{in,3}(f_{IB}) &= G_3(f_{OOB}) V_{out}^3(f_{OOB}) + G(f_{IB}) V_{out,3}(f_{IB}) \\ V_{out,3}(f_{IB}) &= -A_3 V_{in}^3(f_{OOB}) - A V_{in,3}(f_{IB}) \end{aligned} \tag{3.30}$$

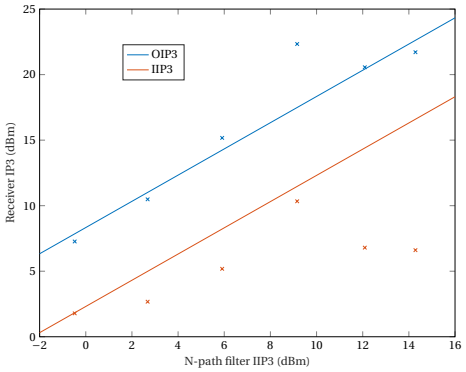

(a) Receiver linearity versus filter linearity. The amplifier is perfectly linear.

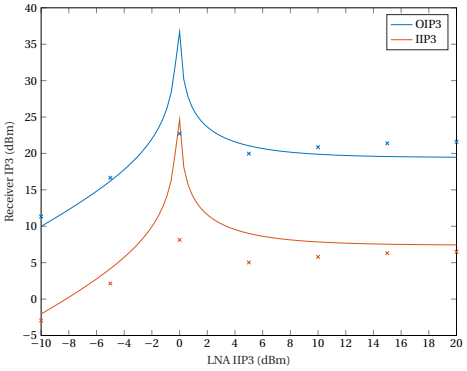

(b) Receiver linearity versus amplifier linearity. The N-path filter has μm wide switches, resulting in an IIP3 of 24 dBm.

Figure 3.13: Linearity of an LNA-first receiver with a notch N-path filter in the feedback path. The voltage gain of the amplifier is 10.

$$V_{out,3}(f_{IB}) = \left(\frac{1}{AG(f_{OOB})}\right)^3 \frac{A^4 G_3(f_{OOB} - A_3}{1 + AG(f_{IB})} V_S^3 \tag{3.31}$$

Knowing the third order voltage, the IIP3 can be calculated. The results are shown in equation 3.32

$$IIP3 = 10log_{10}\left(\frac{v_{out}(f_{OOB})v_{in}^2(f_{OOB})}{v_{out,3}(f_{IB})}\right) = 10log_{10}\left(\frac{1 + AG(f_{IB})}{\frac{A_3}{A} - A^3 G_3(f_{OOB})}\right) \tag{3.32}$$

The contributions of the amplifier and the filter can be split, assuming the contribution of one is much larger than the other. Equation 3.33 shows the two resulting equations.

$$\begin{aligned} IIP3_{rec,A} &= 10log_{10}\left(\frac{1 + AG(f_{IB})}{A^3 G_3(f_{OOB})}\right) \\ &= IIP3_G + 10log_{10}(G(f_{OOB}) - 30log_{10}(A) + 10log_{10}(1 + AG(f_{IB})) \\ IIP3_{rec,G} &= 10log_{10}\left(\frac{1 + AG(f_{IB})}{\frac{A_3}{A}}\right) \\ &= IIP3_A + 10log_{10}(1 + AG(f_{IB})) \end{aligned} \tag{3.33}$$

The results are shown in equation 3.32. This equation shows that the non-linearity of the filter is multiplied by the gain of the amplifier to the third power, compared to the linearity of the amplifier. Therefore, the receiver IIP3 is likely dominated by the filter, except in cases where the amplifier is very non-linear. All non-linear contributions are suppressed by the in-band loopgain $(1 + AG(f_{IB}))$. However, since $G(f_{IB})$ is very small, this does not improve the linearity much.

A receiver with this architecture was simulated in the same way as the LNTA-first receiver. The voltage gain of the amplifier is 10. This results in an out-of-band suppression of 8 dB, for a notch filter with 32um wide switches. The amplifier and filter are matched to 50 ohm. The plots from Figure 3.13 show that the model matches the simulation data. Compared to the bandpass architectures, this setup attenuates the blocker at the antenna level, so the amplifier does not have to amplify a very large blocker signal. This improves the receiver linearity above the linearity of the amplifier and filter on their own.

3.4.3. BANDPASS COMMON GATE ARCHITECTURE

Lastly, the BPCG is analysed. First, the gains from the input to each node are calculated in equation 3.38.

$$V_{in}(f) = \frac{1}{2 + A_1 A_2 G(f)} V_S \tag{3.34}$$
$$V_{A_1}(f) = A_1 V_{in}(f) \tag{3.35}$$
$$V_G(f) = A_1 G(f) V_{in}(f) \tag{3.36}$$
$$V_{A_2}(f) = -A_1 A_2 G(f) V_{in}(f) \tag{3.37}$$
$$I_{g_m}(f) = g_m(1 + A_1 A_2 G(f)) V_{in}(f) \tag{3.38}$$

Next, the equations for the 3rd order tone are set up for each node (equation 3.43). Again, the non-linear gains are derived from the IIP3 using equation 3.29. The total IM3 tone at the input node is found by by combining these equations, resulting in equation 3.44. From this equation the IIP3 is calculated, as shown in equation 3.45.

$$V_{in,3}(f_{IB}) = -R_S I_{g_m,3}(f_{IB}) \tag{3.39}$$
$$V_{A_1,3}(f_{IB}) = A_1 V_{in,3}(f_{IB}) + A_{1,3} V_{in}(f_{OOB})^3 \tag{3.40}$$
$$V_{G_3}(f_{IB}) = G(f) V_{A_1,3}(f_{IB}) + G_3 V_{A_1}(f_{OOB})^3 \tag{3.41}$$
$$V_{A_2,3}(f_{IB}) = -A_2 V_{G_3}(f_{IB}) - A_{2,3} V_G(f_{OOB})^3 \tag{3.42}$$
$$I_{g_m,3}(f_{IB}) = g_m(V_{in,3}(f_{IB}) - V_{A_2,3}(f_{IB})) + g_{m,3}(V_{in}(f_{OOB}) - V_{A_2}(f_{OOB}))^3 \tag{3.43}$$

$$V_{in,3}(f_{IB}) = -\frac{A_2 G(f_{IB}) A_{1,3} + A_1^3 A_2 G_3(f_{OOB}) A_1^3 G_(f_{OOB})^3 A_{2,3} + R_S(1 + A_1 A_2 G(f_{OOB}))^3 g_{m,3}}{2 + A_1 A_2 G(f_{IB})} V_{in}(f_{OOB})^3 \tag{3.44}$$

$$\begin{aligned} IIP3 =& 10log_{10}\left(\frac{V_{in}(f_{OOB})^3}{V_{in,3}(f_{IB})}\right) \\ =& 10log_{10}\left(\frac{2 + A_1 A_2 G(f_{IB})}{A_2 G(f_{IB}) A_{1,3} + A_1^3 A_2 G_3(f_{OOB}) A_1^3 G_(f_{OOB})^3 A_{2,3} + R_S(1 + A_1 A_2 G(f_{OOB}))^3 g_{m,3}}\right) \end{aligned} \tag{3.45}$$

Because $G(f_{IB})$ is very small and because $A_1 A_2 G(f_{OOB})$ is much larger than 1, the numerator of equation 3.45 can be simplified to $2A_1 A_2 G(f_{OOB})$. This simplified equation can be separated into four equations for each of the sources of non-linearity, by assuming for each source that the other sources are negligible. The nonlinear gains are replaced by the IIP3 of the corresponding device, using equation 3.29.

$$\begin{aligned} IIP3_{rec,A_1} =& IIP3_{A_1} + 10log_{10}\left(\frac{G(f_{OOB})}{G(f_{IB})}\right) \\ IIP3_{rec,A_2} =& IIP3_{A_2} - 20log_{10}\left(A_1 G(f_{OOB})\right) \\ IIP3_{rec,G} =& IIP3_G - 20log_{10}\left(A_1\right) \\ IIP3_{rec,g_m} =& IIP3_{g_m} - 20log_{10}\left(A_1 A_2 G(f_{OOB}\right) \end{aligned} \tag{3.46}$$

The non-linearity contributions of the blocks are scaled by different factors. Because the in-band gain of the filter is close to zero, and the out-of-band gain is close to 1, the scaling factor for $A_{1,IM3}$ is very small. This

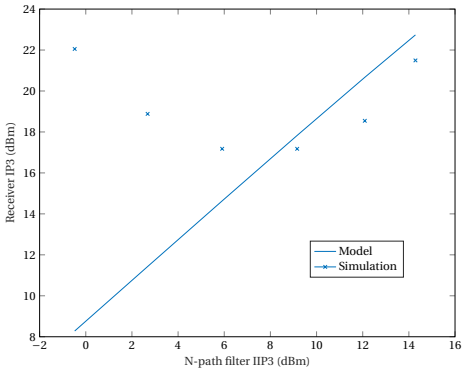

(a) Receiver linearity versus filter linearity. The amplifier is perfectly linear.

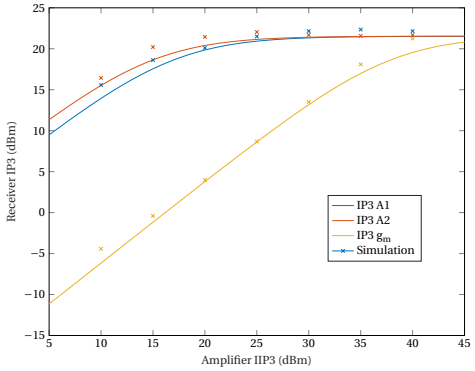

(b) Receiver linearity versus amplifier linearity. N-path filter has 32 μm wide switches, resulting an IIP3 of 24 dBm.

Figure 3.14: Linearity of A BPCG receiver with a notch N-path filter. The amplifier voltage gain is 10.

means that the linearity of A_1 does not influence the receiver linearity much. Its IM3 tone is suppressed by the filter. In contrast, the scaling factor of the non-linearity of the last stage (g_m) is large ($(A_1 A_2 G(f_{OOB}))^2$). It receives the largest amplitude signals at the input because it is the last device in the amplifier chain. This is unavoidable, because it is related to the second order of the out-of-band suppression, which is approximately $A_1 A_2 G(f_{OOB})$. However, there is some room for optimization regarding the non-linear contributions of the other components. A_1 should be small while A_2 provides most of the required gain. This causes a large signal swing at the output node of A_2 (and the input of g_m), while the swing at other nodes is small. To minimize LO leakage however, it is better to have smaller A_2, because the leaked LO is amplified by this amplifier and fed back to the input by the common gate stage.

The BPCG was simulated in the same way as the other receiver architectures. The g_m block has a transconductance of 20mS to match the 50 ohm input. The gain of A_1 is 1 and the gain of A_2 is 10. With an N-path notch filter with 32μm switches, this gives an out-of-band suppression of 10 dB. Figure 3.14a shows the relation between receiver linearity and filter linearity. As before, the receiver linearity is swept by changing the switch width, which also has other effects. Most notably, smaller switches increases the out-of-band loss in the filter. These effects also influence the receiver linearity, explaining the bad fit between model and simulation. From Figure 3.14b it becomes clear that the g_m contributes the most to receiver non-linearity, as predicted by the model. The contributions of A_1 and A_2 are very similar.

3.4.4. CONCLUSION

The receiver architectures based on bandpass N-path filters offer few opportunities for designing a highly linear receiver. Only increasing the width of the switches improves linearity in these circuits. Using a notch N-path filter in the feedback path of an amplifier is more advantageous, because increasing the amplifier gain suppresses the blocker at the input. Still, the filter needs relatively large switches for low out-of-band loss because it is directly connected to the (50 Omega) antenna. The bandpass common gate architecture does not have this issue. This architecture is used as the basis of the receiver design.

3.5. CIRCUIT DESIGN

In order to design a very linear receiver, it is not enough to have a very linear N-path filter. As shown in the previous section, the gain blocks also play a very important role. If the linearity of these blocks is not taken into account, the receiver linearity will be dominated by the gain non-linearity. The design needs a technique to improve the linearity of CMOS gain structures. This is done by IM3 compensation, also called derivative superposition [13]. The amplifiers of the receiver are implemented as inverters. Because an inverter has a very high output impedance, some of the amplifiers have a feedback resistor. The output g_m stage is also im-

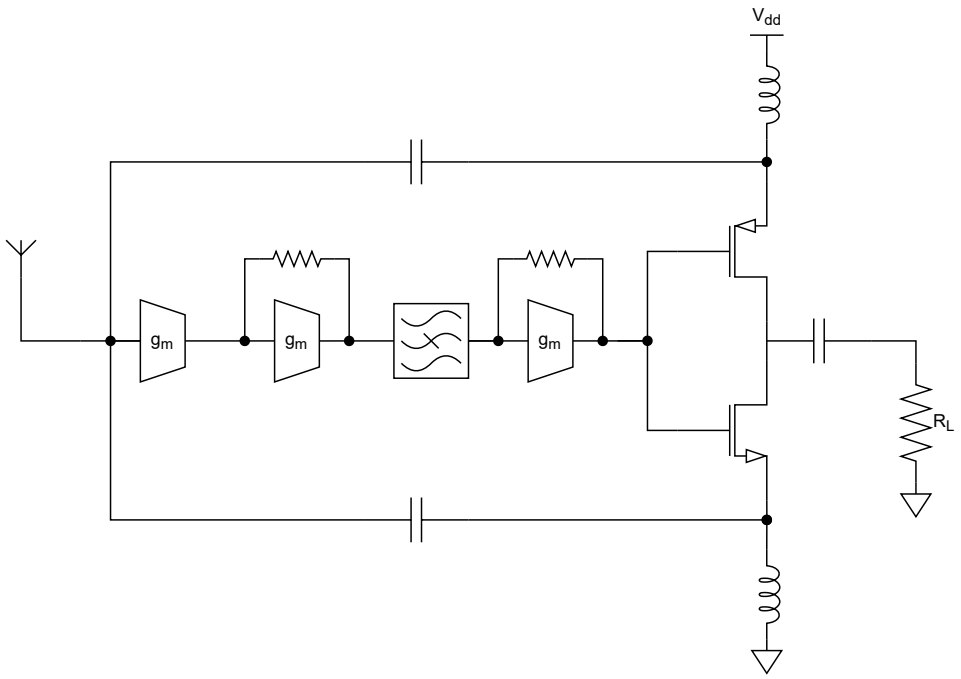

Figure 3.15: Bandpass common gate receiver architecture

plemented by an inverter. It has inductors connecting the source to the bias voltages so it can simultaneously be used as an common-source stage. Figure 3.15 shows the complete receiver schematic.

3.5.1. COMMON GATE FEEDBACK BLOCK

The common gate (CG) feedback block has 2 functions: provide matching for the antenna for wanted signals, and sink blocker current, decreasing their amplitude. It needs to be very linear because it it directly attached to the antenna. Its linearity directly influences the receiver linearity. In order to achieve high linearity the derivative superposition method can be used. In addition to a self-biased inverter, an inverter with different bias voltages is used. Figure 3.16 shows the diagram of this circuit. The transistors on the left form a self-biased inverter, while the transistors on the right form an inverter with adjustable gate bias voltage. Because signals are injected at the source, which is matched to 50 ohm, the circuit needs large inductors. These inductors can not be on chip because of their size.

IM3 COMPENSATION

For the IM3 compensation to work, several criteria must be met. Neglecting the contributions by non-linear capacitances, the transistor's source of non-linearity can be derived from its transconductance curve. The 3rd order derivative of this curve crosses zero. This means there is a bias region where the non-linear contribution is out-of-phase with the signal, and a region where it is in-phase. This is mostly dependent on the gate voltage. This fact can be used to compensate IM3 generated in the receiver. By biasing all inverters in the region where they generate in-phase IM3, this IM3 can be compensated by a single inverter generating out-of-phase IM3. In this design, this is done in the CG stage because it has the largest influence on the linearity of the receiver. The IM3 cancellation in the CG stage can cancel its own non-linearity, but it can also cancel IM3 tones from other parts of the receiver, such as the N-path filter or the amplifiers.

Because an ordinary inverter is biased at half the supply voltage, this has consequences for the supply voltage that can be used. A low supply voltage will cause all inverters to generate in-phase IM3, while a high supply will cause all inverters to generate out-of-phase IM3. Figure 3.17 shows the transfer between these two

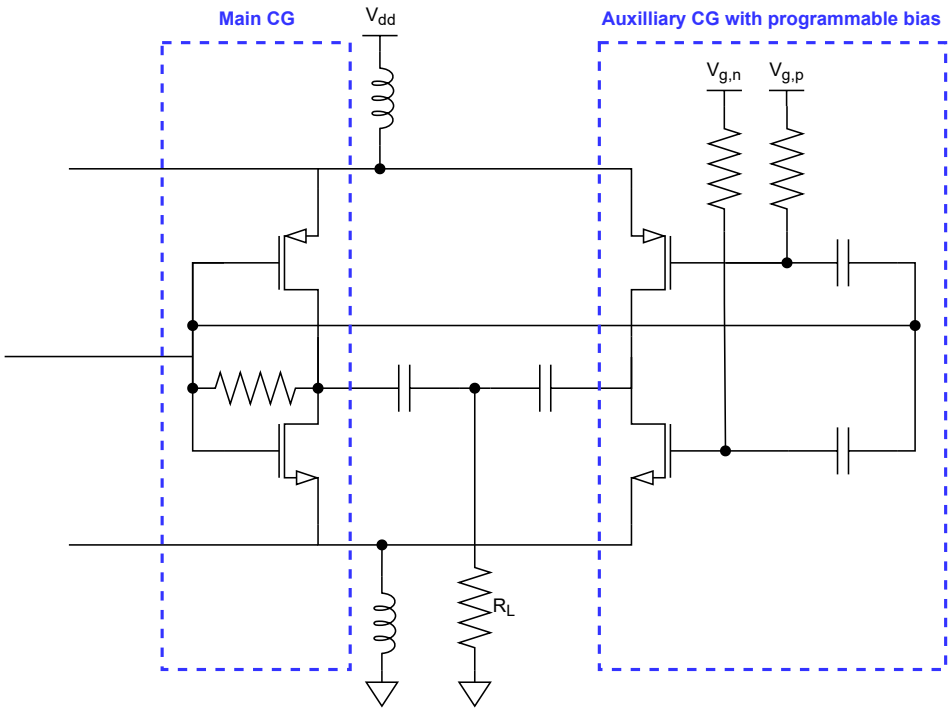

Figure 3.16: Common gate feedback block with IM3 compensation

regions. For this design, a lower supply voltage was chosen (1 Volt), where all inverters generate very low in-phase IM3. This is then compensated by a single inverter with high V_G, generating a large IM3 tone relative to its size.

The IM3 compensating inverter needs a precise bias voltage. This voltage also needs to be adjustable, because production variation can greatly influence the total IM3 that needs compensating. To accomplish this, a bias circuit was designed which can be adjusted with an external current. This current generates the NMOS bias voltage. The PMOS bias voltage is produced by a feedback circuit, which keeps the drain voltage of the inverter close to a reference (half the supply voltage). This feedback circuit needs high gain, but can be very slow. It has a large capacitor to limit the bandwidth and prevent oscillation. Figure 3.18 shows the complete circuit with the inverter it is biasing. The function of the adjust current is shown in Figure 3.19a. Figure 3.19b shows the loop gain and loop delay. For this simulation, the loop is opened at V_D and a voltage is applied at input of the bias circuit. The response is measured at the output of the inverter. The system is stable, the gain margin is 20 dB and the phase margin is 54 degrees.

3.5.2. GAIN BLOCKS

The gain blocks have two functions. The most important function is to provide gain to the feedback stage to reject blockers. This also includes extra gain to negate the filter out-of-band loss. The second function is to isolate the input, feedback stage and filter from each other. This will ensure that the filter response is not too much affected by loading impedances.

The feedback gain must be negative. Therefore, 3 inverters are used. The first inverter provides gain and prevents the filter from loading the input. The last inverter prevents the CG feedback block from capacitively loading the filter. The second inverter is added after the first, to provide a lower driving impedance to the filter and further increase gain. Figure 3.15 shows the bandpass common gate architecture with the three inverters.

The second inverter drives the filter. It needs a stable, resistive output impedance. For that purpose the

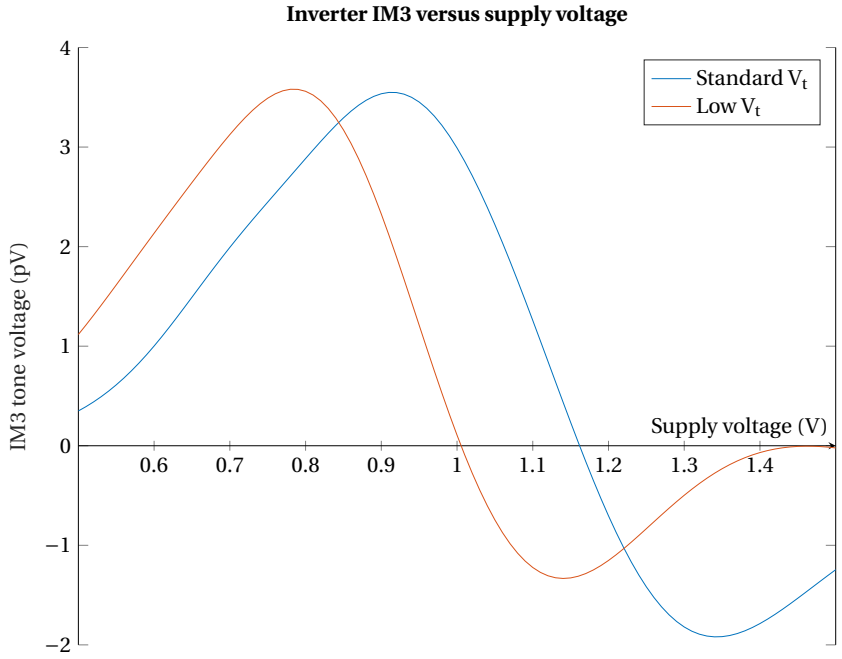

Figure 3.17: Inverter IM3 versus supply voltage. Inverter consists of 40 nm length, 8μm NMOS and 16 μm PMOS transistor, driven by 10 kΩ source and drives a 25 Ω resistor. IM3 is measured at output. Two tone test tones at 1.1 GHz and 1.2 GHz, -30 dBm power.

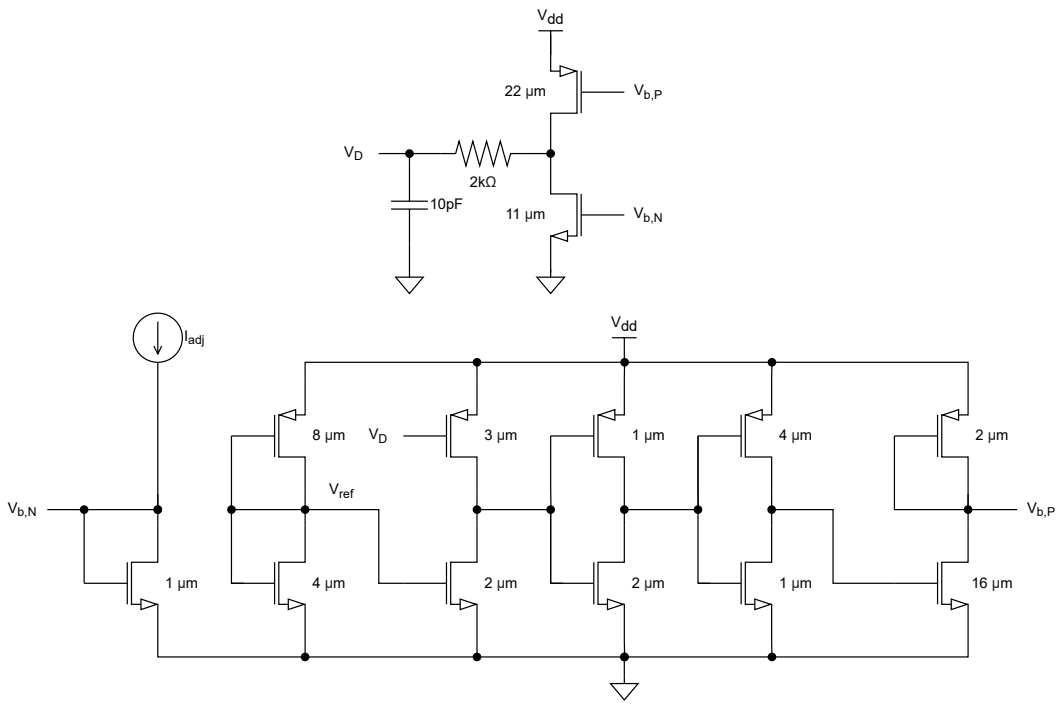

Figure 3.18: Bias circuit for IM3 compensating common gate. All transistors are minimum length (40 nm)

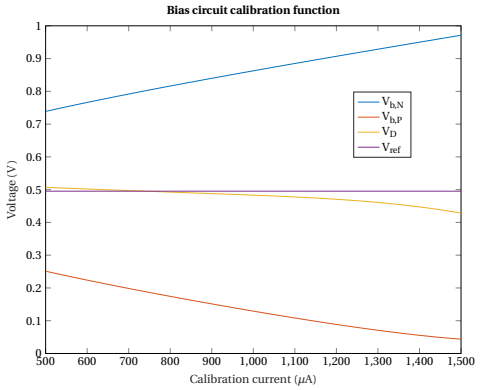

(a) Effect of the adjust current on the NMOS and PMOS bias voltages

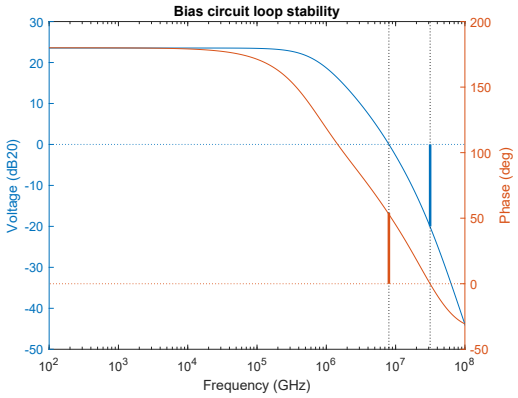

(b) Loop stability of the bias circuit, measured at V_D

Figure 3.19: Bias circuit simulation results

inverter is used as a transimpedance amplifier (TIA) with a 1.2 kΩ resistor in the feedback path. This provides around 400 Ω output impedance.

The third inverter is driving the common gate stage. Its output impedance influences the linearity of the CG stage, and thus the linearity of the receiver. The IM3 compensation of the CG stage only works if the linearity of the components is constant. Therefore, the output impedance of the third inverter also needs to be stable. This inverter is also used as a transimpedance amplifier with a 5 kΩ resistor in the feedback path.

Because the feedback block is able to correct for 3rd order non-linearity, the linearity of these blocks does not need particular attention. As long as the supply voltage is set such that an inverter generates minimal in-phase IM3, the feedback stage can compensate for this non-linearity.

3.5.3. N-PATH NOTCH FILTER

The N-path filters linearity is dependent on the switch sizes and source- and load impedances. Increasing the switch size improves linearity and reduces losses caused by switch on-resistance up to a certain point. This is explored in section 3.3.1. There are two notch filter structures that can be used. The typically used N-path notch structure has one capacitor in series with two switches for each phase. It is also possible to use only one switch, but then the parasitic capacitances will load the input or output. This can cause problems when the capacitive loading introduces too much delay in the feedback loop, degrading loop stability and risking oscillation in the circuit. Therefore, the structure with two switches is used.

The input and output of all the inverters in the design are biased at half the supply. To save coupling capacitors, it is preferable that the filter works with the signals biased at the same voltage. This is possible by using a bias level shift circuit to drive the gates of the NMOS switches. Figure 3.20 shows the schematic. The resistors bias the transistor gate such that V_{GS} of the switching transistor is equal to V_{LO}.

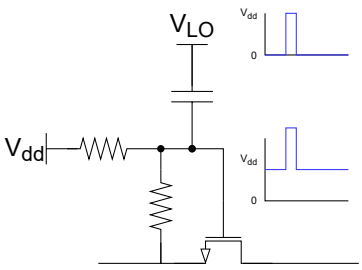

Figure 3.20: N-path gate bias circuit

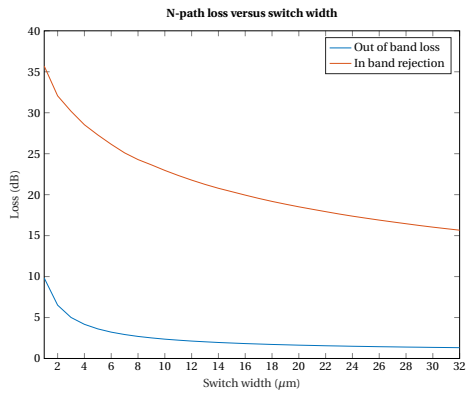

(a) N-path notch filter out-of-band loss versus switch width

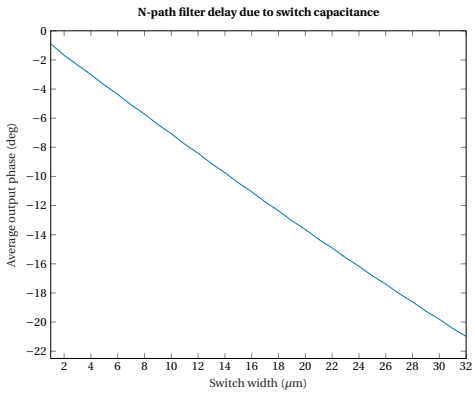

(b) N-path notch filter out-of-band phase delay versus switch width

Figure 3.21: N-path notch filter delay and loss versus switch width

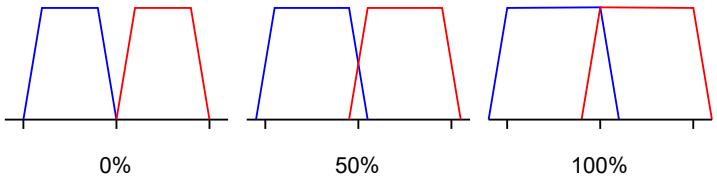

Figure 3.22: Switching signal overlap in the transition period

An important parameter of the filter, besides the capacitance, is the switch size. A larger switch means lower R_{on} and thus lower losses, but also more parasitic capacitance. If this capacitance is too large, it will introduce leakage of the in-band signal, degrading the rejection. Besides that, the parasitic capacitance creates delay, which can degrade the stability of the loop [14]. To find a good switch size, the N-path filter was simulated with different switch sizes. Figure 3.21a shows that out-of-band loss decreases with switch size, and in band rejection degrades logarithmically with switch size. The phase delay scales linearly with switch size (figure 3.21b). For acceptable losses, good rejection, and little delay, a switch size of 8um was chosen.

The LO signals driving the switches are assumed to be high or low in the analysis. In reality however, the transition between these two states takes time. For a 20 pS/V slew rate and a 1 V LO signal this takes 20 pS. Therefor, there can be some overlap during the transition without any two switches being fully on at the same time. Figure 3.22 shows this visually.

No overlap means smaller pulses, which will increase losses of the filter. Also, when all the switches are off, the impedance presented to the input of the filter is different. Together with charge from the gate-source capacitances, this creates a signal at the LO frequency. This signal is most prominent at $N \cdot f_{LO}$ and its harmonics. The optimum overlap is when at all times exactly one switch is on. This depends of course on the LO voltage and the NMOS threshold voltage. The overlap was optimized with regards to LO leakage using simulation. The simulated filter has 8 paths, a switching frequency of 1 GHz and 1 pF capacitance per phase. The input and output are terminated with 400 Ω resistors and biased at 500mV. Minimum length low threshold voltage (LVT) switches were used, 8mum wide. Figure 3.23a and 3.23b show that regardless of the slope of the switching signal, the optimum overlap is around 55%.

3.5.4. SIMULATION RESULTS

Figure 3.24 shows the transfer function and input reflection coefficient of the designed receiver. The out-of-band signals are suppressed by 10 dB. The bandwidth is 100 MHz. Figure 3.25 shows the range of frequencies the receiver can be set to. The receiver performance for low frequencies is limited by the size of the inductor. For f_{LO} equal to 200 MHz, the matching is not very good (S11 is less than -10dB), as shown in Figure 3.25. At

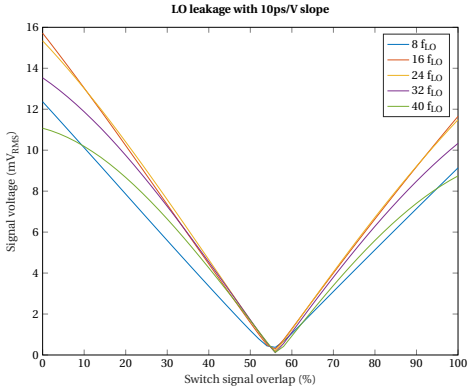

(a) N-path notch LO leakage versus overlap, with 10ps/V slew rate

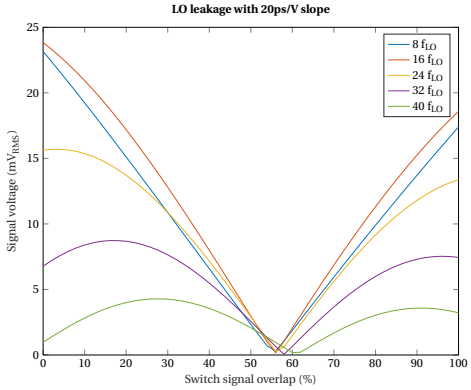

(b) N-path notch LO leakage versus overlap, with 20ps/V slew rate

Figure 3.23: N-path notch LO leakage versus overlap

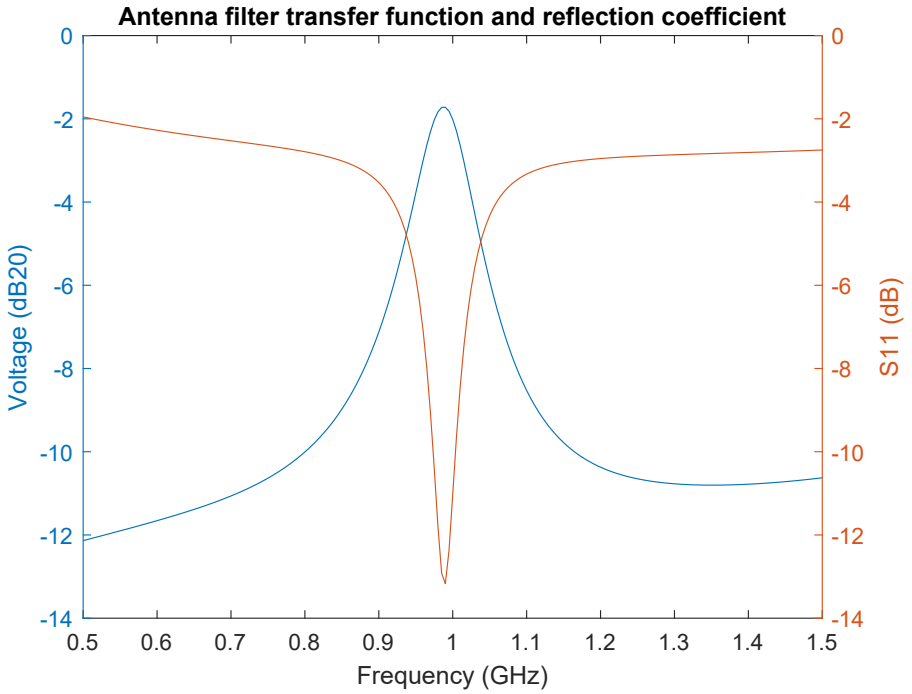

Figure 3.24: Receiver front-end voltage transfer and S11

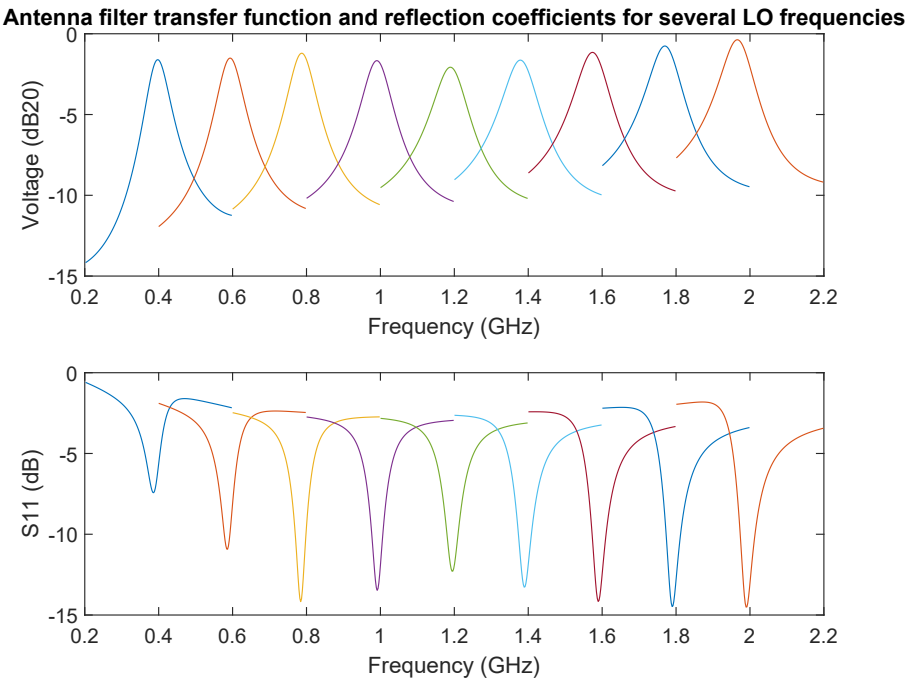

Figure 3.25: Receiver front-end transfer S11 for several LO frequencies

high frequencies, the performance is limited by the parasitic capacitances of the transistors and the inductor.

Figure 3.26 shows the high linearity that can be obtained by calibrating the IM3 cancellation. This simulation was done by presenting two -20 dBm test tones at 1.2 GHz and 1.41 GHz to the receiver, and measuring the IM3 tone. The transistors of the IM3 compensating common gate stage are sized to cancel out-of-band IM3. Therefor, the in-band linearity is not as good and does not change with the bias current.

	This work	Elmi et al.[10]	Lin et al.[11]	Huang et al.[5]	Soer et al.[3]	Andrews et al.[4]
RF input	single ended	single ended	single ended	single ended	differential	single ended
N	8	8	8	8	4	8
Freq. range (GHz)	0.5 - 2	0.1 - 2	0.15 - 0.85	3.7 - 6.5	0.2 - 2.0	0.1-2.4
S11 (dB)	<-10	<-10	-12			-30
OOB-IIP3 (dBm)	29	15.9	17.4	28	11	25
Bandwidth (MHz)	100	1	9		25	20
Supply (V)	1	1.2	1.2 / 2.5		1.2	1.2 / 2.5
CMOS technology	40 nm	90nm	65nm	45nm SOI	65nm	65nm

Table 3.2: Comparison of this work with N-path receivers from recent literature

3.6. CONCLUSION

This works shows that it is possible to design a highly linear receiver with an N-path filter in a 40nm CMOS process, using both the intrinsic linearity of the N-path filter and IM3 cancellation techniques. The design needs a 1 V supply. The amplifiers and common gate stage consume 1.9 mA together, while the bias circuit draws 220 μA. This adds to a total of 2.12 mA. The transistors in the N-path filter are driven by ideal voltage sources in this design, which deliver negligible power. A practical design requires a clock generator and gate drivers, which would consume power.

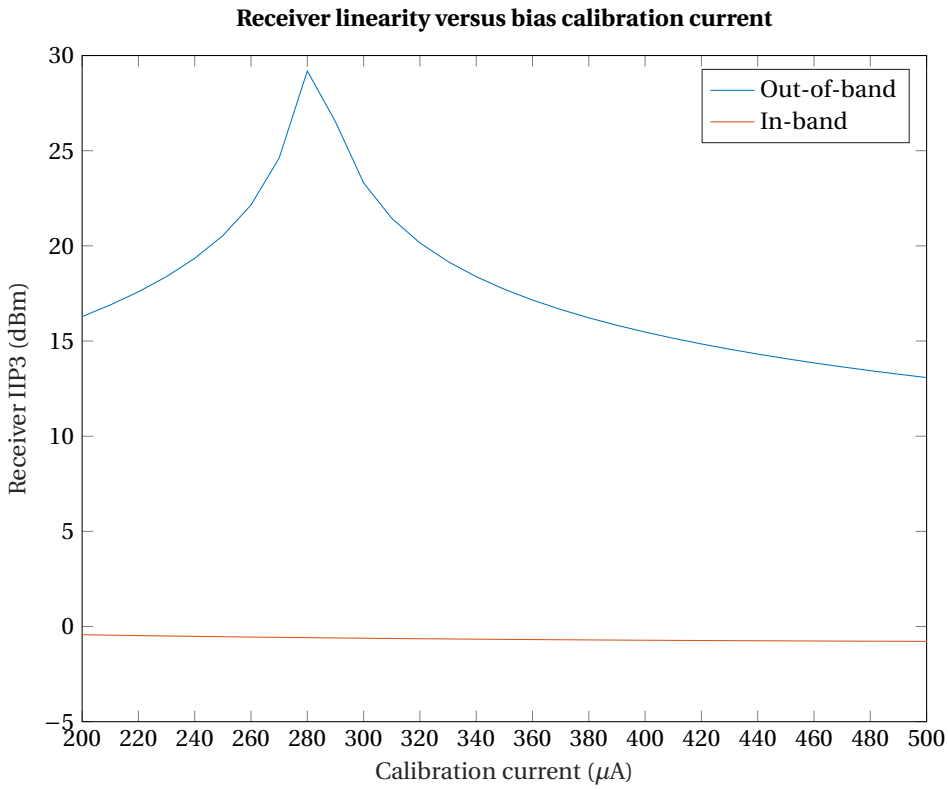

Figure 3.26: Receiver linearity improved by calibrating the IM3 rejecting common gate stage

3.6.1. FUTURE WORK

The filtering obtained by the designed receiver has only a first-order slope. Multiple N-path filters can be combined to obtain a higher order filter. For example, a pi-type bandpass filters can be realized with three N-path filters [14]. This will introduce more delay, so phase compensation techniques could be required to make such a higher order receiver work with the bandpass common gate architecture. The N-path notch filter in [15] uses a different filter architecture. This requires half the number of capacitors as the conventional notch filter, however, the total capacitance is the same for the same filter response. It has the advantage that the filter response is not present on the even harmonics. Implementing this filter with the designed receiver could have some benefits.

A

Design schematic

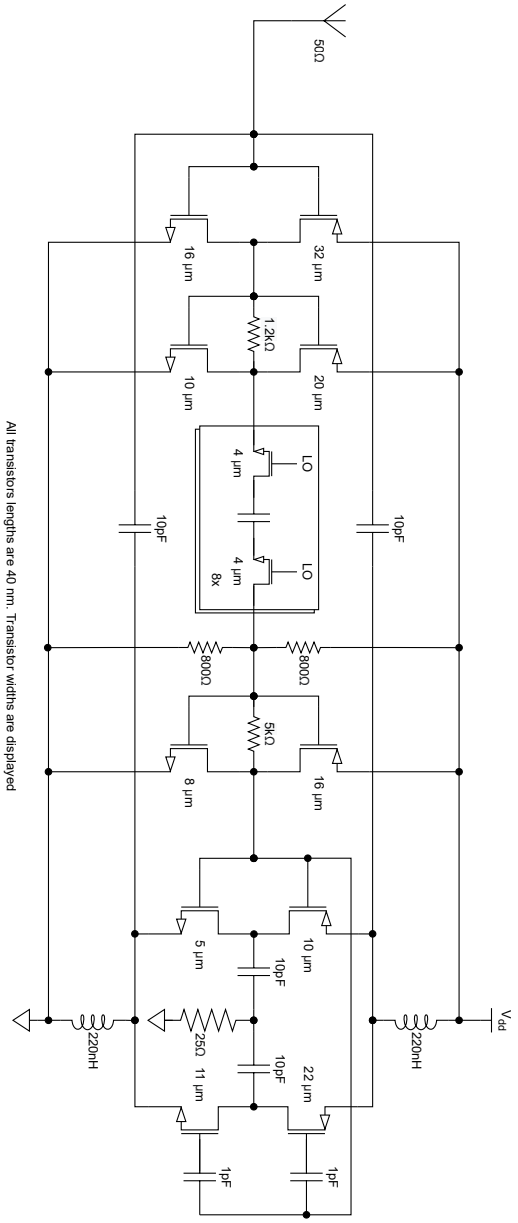

BIBLIOGRAPHY

[1] L. Franks and I. W. Sandberg, *An alternative approach to the realizations of network functions: The n-path filter,* The Bell System Technical Journal **39**, 1321 (1960).

[2] A. Molnar and C. Andrews, *Impedance, filtering and noise in n-phase passive cmos mixers,* in *Proceedings of the IEEE 2012 Custom Integrated Circuits Conference* (2012) pp. 1–8.

[3] M. C. M. Soer, E. A. M. Klumperink, Z. Ru, F. E. van Vliet, and B. Nauta, *A 0.2-to-2.0ghz 65nm cmos receiver without lna achieving >11dbm iip3 and <6.5 db nf,* in *2009 IEEE International Solid-State Circuits Conference - Digest of Technical Papers* (2009) pp. 222–223,223a.

[4] C. Andrews and A. C. Molnar, *A passive mixer-first receiver with digitally controlled and widely tunable rf interface,* IEEE Journal of Solid-State Circuits **45**, 2696 (2010).

[5] S. Huang and A. Molnar, *A 3.7-6.5ghz 8-phase n-path mixer-first receiver with lo overlap suppression achieving 5db nf and 5dbm oob b1db,* in *2021 IEEE Radio Frequency Integrated Circuits Symposium (RFIC)* (2021) pp. 87–90.

[6] M. Mikhemar, D. Murphy, A. Mirzaei, and H. Darabi, *A cancellation technique for reciprocal-mixing caused by phase noise and spurs,* IEEE Journal of Solid-State Circuits **48**, 3080 (2013).

[7] H. Khatri, P. S. Gudem, and L. E. Larson, *Distortion in current commutating passive cmos downconversion mixers,* IEEE Transactions on Microwave Theory and Techniques **57**, 2671 (2009).

[8] W. P. Robins, *Phase Noise in Signal Sources* (Peregrinus, 1982).

[9] A. Mirzaei, H. Darabi, and D. Murphy, *Architectural evolution of integrated m-phase high-q bandpass filters,* IEEE Transactions on Circuits and Systems I: Regular Papers **59**, 52 (2012).

[10] M. Elmi, A. Aghajani, M. J. Nokandi, and A. Jalali, *A wideband receiver front-end using active/passive n-path mixers,* in *2016 24th Iranian Conference on Electrical Engineering (ICEE)* (2016) pp. 1650–1654.

[11] F. Lin, P.-I. Mak, and R. P. Martins, *An rf-to-bb-current-reuse wideband receiver with parallel n-path active/passive mixers and a single-mos pole-zero lpf,* IEEE Journal of Solid-State Circuits **49**, 2547 (2014).

[12] H. Wang, Z. Wang, and P. Heydari, *28.7 a wideband blocker-tolerant receiver with high-q rf-input selectivity and lt;-80dbm lo leakage,* in *2019 IEEE International Solid- State Circuits Conference - (ISSCC)* (2019) pp. 450–452.

[13] A. I. Mecwan and N. M. Devashrayee, *Linearity improvement of lna using derivative superposition: Issues and challenges,* in *2017 7th International Conference on Cloud Computing, Data Science Engineering - Confluence* (2017) pp. 759–763.

[14] M. Darvishi, R. van der Zee, and B. Nauta, *Design of active n-path filters,* IEEE Journal of Solid-State Circuits **48**, 2962 (2013).

[15] M. Khorshidian, N. Reiskarimian, and H. Krishnaswamy, *29.4 high-performance isolators and notch filters based on n-path negative transresistance,* in *2020 IEEE International Solid- State Circuits Conference - (ISSCC)* (2020) pp. 446–448.